Cbl in Epidermal Growth Factor Receptor trafficking

Benedicte Semb Hagen

Thesis for the Master´s degree in Molecular Biosciences

60 study points

Department of Biosciences
Faculty of Mathematics and Natural sciences

University of Oslo

2013

Table of Contents

Acknowledgements

The presented work in this study was performed at Professor Oddmund Bakke´s laboratory at the Department of Biosciences, Faculty of Mathematics and Natural Sciences, University of Oslo, from September 2012 to April 2013.

First, I would like to thank Professor Oddmund Bakke for providing me the opportunity to work as a master student at his lab. Also, I wish to thank all the members of the Bakke lab for giving great scientific advise and being including and altogether providing a good working environment.

A major gratitude to my supervisor Lene E. Johannessen for everything she has taught me, for great advices and for being extremely patient with me. Further, I would like to thank my co-supervisor Catherine Heyward for invaluable help during the last period of this master study and also Frode M. Skjeldal for all technical support.

I want to thank my sister, mum and dad for all support and for believing in me, and also my friends for making sure that I still had a social life and for many laughs. I would also like to thank my fellow students for many valuable discussions and great support. Last, but not least, I wish to thank my dear Espen for all encouragement, wonderful patience and for being there for me.

Oslo, May 2013

Benedicte Semb Hagen

Summary

The Casitas B-lineage lymphoma (Cbl) family of ubiquitin ligases has been studied for years regarding their important role in downregulation of ligand bound epidermal growth factor receptor (EGFR). The two isoforms c-Cbl and Cbl-b share the same structural features and are thought to be equally important for EGFR downregulation. Few comparative studies between c-Cbl and Cbl-b have been published with respect to EGFR regulation. Even though both Cbl proteins appear to display the same functional activity in EGFR regulation, some studies reveal that there might be some differences between these two isoforms. In this study, we have used biochemical studies and live imaging to further investigate and compare the recruitment and intracellular trafficking of c-Cbl and Cbl-b upon EGF stimulation.

Summarized, Cbl-b is recruited more efficiently to EGFR than c-Cbl upon receptor activation. However, this difference in recruitment does not seem to affect their trafficking, as both isoforms follow the same trafficking pattern to early endosomes.

The finding that Cbl-b is recruited to the EGFR more efficiently than c-Cbl is recruited to the EGFR, implies that they could have distinct activities at early time points. Due to their important roles in downregulation of growth factor signaling, further investigations regarding their individual functions are of great importance.

Abbreviations

Cbl	Casitas B-lineage lymphoma
CIN85	Cbl-interacting protein of 85 kDa
DMEM	Dulbeccos Modified Eagles Medium
E1	Ubiquitin activating enzyme
E2	Ubiquitin conjugating enzyme
E3	Ubiquitin ligase
EGF	Epidermal growth factor
EGFR	Epidermal growth factor receptor
ErbB	Epidermal growth factor receptor family of receptor tyrosine kinases
ESCRT	Endosomal sorting complex required for sorting
Grb2	Growth factor receptor-bound protein 2
HECT	Homologous to E6-AP carboxy terminal
Ii	Invariant chain
IP	Immunoprecipitation
kDa	Kilo Dalton
PBS	Phosphate buffered saline
PM	Plasma membrane
PVDF	Polyvinylidene fluoride
pY	Phosphorylated tyrosine
RING	Really-interesting-new-gene
ROI	Region of interest
RT	Room temperature
RTK	Receptor tyrosine kinase
SDS-PAGE	Sodium dodecyl sulphate polyacrylamide gel electrophoresis
SH2	Src-homology 2 domain
SH3	Src-homology 3 domain
TAE	Tris-acetate-EDTA
TBS	Tris-buffered saline
TKB	Tyrosine kinase binding domain
UBA	Ubiquitin associated domain
Wt	Wild type

1 Introduction

1.1 Growth factor receptors

Cells constitute the basic building blocks in every living organism and are dependent on numerous different growth factors in order to maintain normal growth, development and for maintaining homeostasis. In multicellular organisms, these growth factors are especially important signals in cell-to-cell communications during tissue development, cell migration, cell survival and apoptosis in embryogenesis.

Growth factors bind to the extracellular part of specific receptors located in the plasma membrane, which lead to conformational changes and activation of the intracellular part of the receptor. The receptor activation induces specific intracellular signaling pathways dependent on the type of growth factor, which in turn lead a cellular response. The final outcome of the cellular response is dependent on the duration and intensity of the signaling combined with the activity of various signaling proteins involved in these pathways. The activities of the intracellular signaling pathways are carefully controlled by other proteins in order to prevent excessive growth response. Another important mechanism involved in signal attenuation is the removal of the receptor-ligand complex from the cell surface.

Most of these growth factor receptors have a similar molecular structure, with the well characterized receptor family receptor tyrosine kinases (RTKs) as a typical member. The RTKs are transmembrane proteins containing an extracellular ligand binding part and an intracellular tyrosine kinase domain responsible for activation of signaling pathways. These receptors are therefore capable of transforming the extracellular binding of a specific type of growth factor into activation of several specific intracellular signaling pathways. These signaling pathways are carefully regulated, ensuring a controlled cellular response. Dysregulation of growth signals by mutations in RTKs or disturbance in intracellular signaling pathways is implicated in various diseases such as cancer, diabetes and inflammation (Wieduwilt and Moasser, 2008).

The RTKs have been extensively studied for years and have revealed important insights into their structure and regulation. The increased understanding of their nature has been important for the development and improvement of drugs.

1.2 The Epidermal Growth Factor receptor

The epidermal growth factor receptor (EGFR) is one of four members in the epidermal growth factor family of receptor tyrosine kinases (ErbBs), all of which share homologous sequences. The ErbB family consists of the EGFR (ErbB1, HER1), ErbB2 (HER2), ErbB3 (HER3) and ErbB4 (HER4), which are essential in regulating cellular differentiation, proliferation, migration and survival (Wieduwilt and Moasser, 2008). They are one of at least 58 discovered human members of transmembrane RTKs, which all share a conserved structure and function and are necessary for regulating normal cellular processes (Lemmon and Schlessinger, 2010).

EGFR is expressed in cells with epithelial, mesenchymal and neuronal origin and is important for regulating cell development, proliferation, migration and for maintaining homeostastis (Yano et al., 2003). It is distributed on the basolateral surface on epithelial cells where it is are able to bind secreted ligands exclusively on this side. In this way, the receptor can interact with growth factors promoting cell proliferation and migration, both processes required for wound healing. Also, the tight junctions between the epithelial cells creates a barrier towards growth factors that are secreted onto the apical side. If this barrier is broken, for instance by a wound, growth factors gain access to receptors on the basolateral side. When the barrier is restored due to epithelial growth, the wound is healed and growth factors can no longer access the receptors (Vermeer et al., 2003)**.** This asymmetrical distribution contributes to the polarization in the epithelial cell, which is important for the directional transport of molecules. Loss of polarity is often implicated in epithelial cancers, giving EGFR access to apically located growth factors. This in turn may result in sustained or prolonged growth signaling and thus uncontrolled cell migration or cell proliferation (Casaletto and McClatchey, 2012).

Normally, the cell density and amount of cell-to-cell contact regulates the activity of EGFR and in this way also controls the epithelial tissue growth (Kim et al., 2009). Knockout of EGFR has been reported to result in embryonic lethality in mice (Threadgill et al., 1995) and

deficient development of epithelial tissues in many vital organs (Miettinen et al., 1995; Sibilia and Wagner, 1995). Mutations or dysregulation of EGFR is also involved in the development of colorectal cancer (Krasinskas, 2011), non-small-cell lung cancer (Gorgoulis et al., 1992), head and neck cancer (Irish and Bernstein, 1993) and glioblastomas (Wong et al., 1992).

EGFR has been studied for decades and has become the receptor model for studying mechanisms underlying receptor tyrosine kinase signaling and signaling attenuation. Correct attenuation of receptor signaling is crucial for controlled cell growth. One important regulatory mechanisms is to rapidly remove the receptor from the plasma membrane by endocytosis, a mechanism involving many adaptor proteins and enzymes (Casaletto and McClatchey, 2012). Among these is the ubiquitin ligase Casitas B-lineage lymphoma (Cbl) family that attaches ubiquitin onto lysine residues in the cytoplasmic tail of the receptor, a modification that further recruits other adaptor proteins and targets the receptor for internalization and transport to lysosomes for degradation. Also, recent studies of EGFR structure and behavior have gained additional knowledge that facilitates the development of new cancer drugs (Endres et al., 2011).

1.2.1 EGFR structure

The ErbB familyof receptors are all transmembrane proteins, consisting of an extracellular glycosylated N-terminal domain containing ligand binding sites and cysteine-rich domains for dimerization, a transmembrane section, a small juxtamembrane segment, and an intracellular C-terminal domain containing a number of tyrosine phosphorylation (pY) sites and a tyrosine kinase domain (Bazley and Gullick, 2005) (figure 1-1).

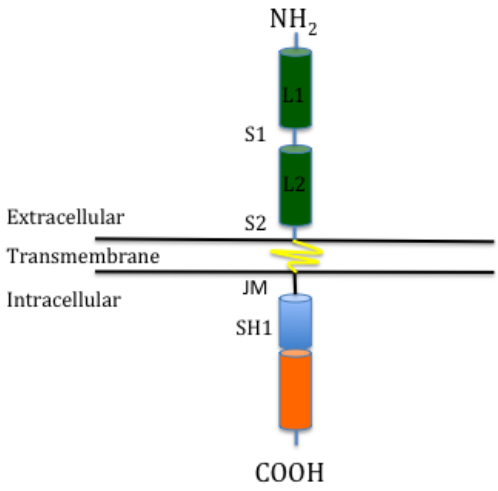

Figure 1-1. ErbB receptor structure. The ErbB receptor family are transmembrane proteins with an extracellular N-terminal domain, a transmembrane domain, a small juxtamembrane domain (JM), and a C-terminal cytoplasmic part. The N-terminal part contains ligand binding sites (L1/L2) and cysteine residues (S1 and S2), S1 are invloved in EGFR dimerization. The C-terminal domains consists of a protein kinase domain (SH1) and tyrosine residues that become phosphorylated upon receptor activation (orange part). Modified from (Bazley and Gullick, 2005)

EGFR is the only member of the ErbB famliy which is capable of rapid ligand-induced endocytosis (Baulida et al., 1996). Seven different ligands can bind to the EGFR (Hynes and MacDonald, 2009) and they all induce internalization from the plasma membrane (PM). However, after internalization from the PM each of them triggers different mechanisms of intracellular sorting of the receptor, either to the recycling or the degradative pathway. Ligands which dissociate from the receptor in early endosomes induce receptor recycling (transforming growth factor-α (TGF-α), epiregulin (EPI), amphiregulin (AR)), whereas others that remain bound lead to further receptor sorting to lysosomes for degradation (EGF, heparin-binding EGF (HB-EGF), betacellulin (BTC)) (Roepstorff et al., 2009). Of these ligands, EGF has been the most used ligand when studying trafficking and downregulation of EGFR, as it is the founding member of the EGF family of proteins (Carpenter and Cohen, 1979).

1.2.2 EGFR activation and signaling

Upon binding of EGF, the EGFR forms an asymmetric kinase dimer leading to activation of the tyrosine kinase domain. This event induces transphosphorylation of tyrosines in the cytoplasmic tail, by which a specific tyrosine kinase domain in one of the receptors (activator kinase) bind to the head of the other tyrosine kinase domain (receiver kinase). This in turn leads to a conformational change where the receiver kinase phosphorylates tyrosines both on its own tail and the dimerization partner (figure 1-2) (Endres et al., 2011).

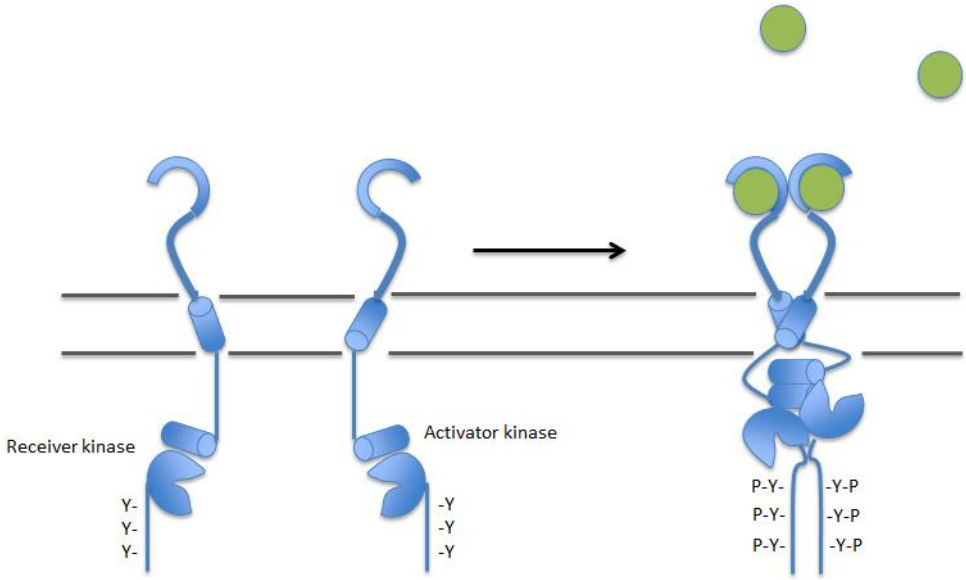

Figure 1-2. EGF receptor activation. In the inactivate state, EGFRs are mainly distributed as monomers across the cell membrane. Upon ligand binding, the receptors dimerize in an asymmetric manner leading to activation of the intrinsic tyrosine kinase activity and autophosphorylation of distinct tyrosine residues in the cytoplasmic tail.

This autophosphorylation event creates binding sites for proteins containing phosphoryrosine binding domains, such as the Src-Homology 2 (SH2)-domain. Two of the major proteins recruited to the phosphotyrosine sites are the adaptor protein growth factor receptor-bound protein 2 (Grb2) and Shc. Grb2 is fast recruited to pY1068 and pY1086 in the cytoplasmic tail of the EGFR upon its activation, at which it binds through its SH2 domain. Grb2 is also bound to and recruits to the EGFR Son-of-Sevenless (SOS), a Ras a guanine-exchange factor that activates Ras GTPase located at the PM. Grb2 may also bind to the receptor indirectly by associating with Shc through its SH3 domain, at which Shc binds directly to phosphotyrosine

residues through its SH2 domain. Activation of Ras leads to activation of the well characterized mitogen-activating protein kinase (MAPK)/extracellular signal-regulated kinase (ERK) signaling pathway which ultimately regulates DNA transcription. Additionally other signaling pathways are induced upon EGFR activation, such as PI3P/Akt signaling that regulates cell proliferation and survival. At the same time, Grb2, which is involved in signal transduction, also induces receptor internalization by recruiting proteins responsible for receptor endocytosis (Schlessinger et al., 1983; Sorkin and von Zastrow, 2009; Yarden and Schlessinger, 1987a; Yarden and Schlessinger, 1987b). The type of ligand binding to the EGFR determines the sites of autophosphorylation, which in turn regulates the activation of specific signaling proteins and ultimately regulation of gene expression and thus cellular response (Olayioye et al., 1998). Figure 1-3 illustrates the major signaling pathways initiated by the ligand bound activated receptor.

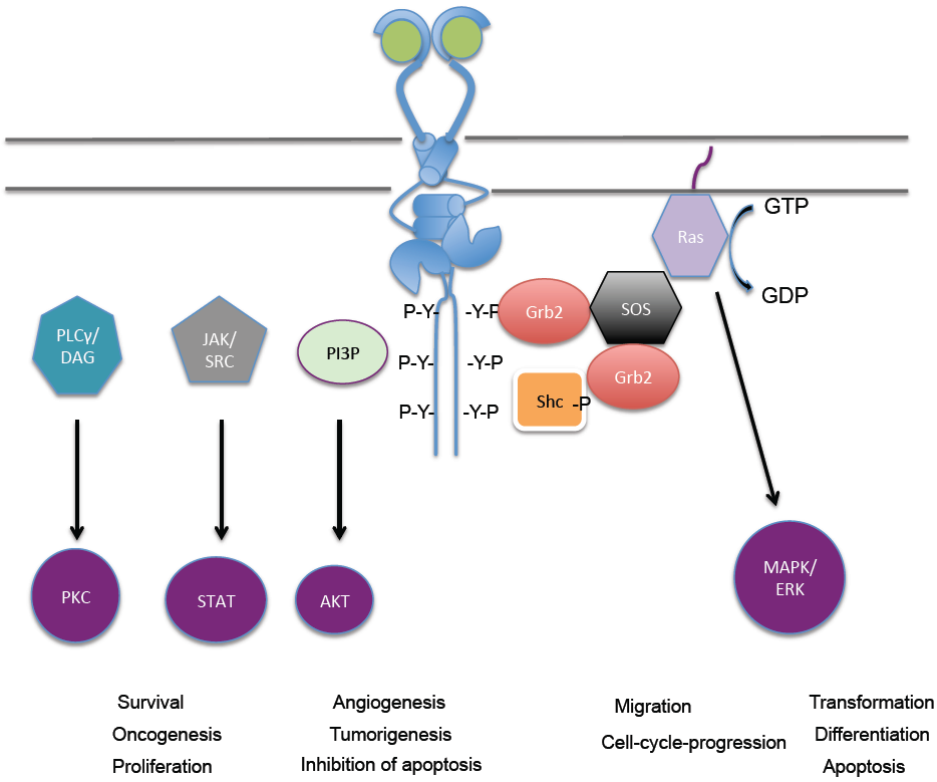

Figure 1-3. EGFR signaling. Upon receptor activation by ligand binding, the receptor initiates downstream signaling by recruiting several effector proteins involved in different signaling pathways ultimately leading to specific cellular responses.

Activated, ligand bound EGFR continues to induce intracellular signaling on endosomes as long as it exists in a phosphorylated state, sustaining the interaction with effector proteins such as Grb2, Shc and SOS. Thus, peristent EGF receptor signaling both from the PM and on endosomes could ultimately lead to uncontrolled cell growth and proliferation. Attenuation of signaling is controlled by receptor modification by ubiquitin, receptor dephosphorylation and ligand dissociation at the lower pH found in later endosomes (Lai et al., 1989; Sorkin and Carpenter, 1991).

1.3 Endosomal trafficking

Endocytosis is a general term for the cellular uptake and intracellular sorting of extracellular material, such as nutrients, cell surface receptors, plasma membrane lipids and other soluble particles. Several uptake mechanisms have been identified, depending on the type of cargo (Scita and Di Fiore, 2010). A well-studied endocytic route is clathrin-mediated endocytosis, where extracellular cargo is selected by adaptor proteins into specialized areas at the PM called clathrin coated pits followed by intracellular transport in clathrin coated vesicles. Clathrin-mediated endocytosis is described as the main endocytic route, especially for the internalization of plasma membrane receptors (Doherty and McMahon, 2009). Clathrin and adaptor protein 2 (AP2) are the main components in the clathrin coated pits. The uptake of extracellular cargo through this route is initiated by the cooperation of adaptor proteins which recognize and bind the cargo and lastly recruit clathrin triskelia to coat the forming clathrin coated pit at the PM. AP2 or other cargo-specific adaptor proteins, are responsible for the recognition and binding of cargo, and further recruit clathrin triskelia from the cytosol to areas containing adaptor proteins. The clathrin polymerization leads to stabilization of the membrane curvature, assisted by other adaptor proteins, like the epsins. The membrane scission is mediated by the enzymatic activity of dynamin. After budding from the plasma membrane, other adaptor proteins such as auxillin or G-associated kinase, recognizes clathrin inducing dissociation and recycling of clathrin, which lastly produces a cargo-containing endosome (McMahon and Boucrot, 2011).

Once internalized, extracellular cargo enters early endosomes and becomes further sorted to distinct destinations, such as lysosomal degradation, recycling to the plasma membrane or retrotransport to Golgi, all depending on the type of trafficking route they encounter. The sorting processes during endosomal pathways are highly dynamic and complex, where

effector proteins on the early endosome determine the fate of the cargo (Sigismund et al., 2012).

1.3.1 Endosomal trafficking of EGFR

Clathrin-mediated endocytosis is considered to be the most common endocytic route of the EGFR, although other endocytic pathways have been suggested. The type of uptake of the receptor depends on the ligand concentration: lower ligand concentrations favor clathrin mediated endocytosis and higher concentrations favor clathrin independent endocytosis (Goh et al., 2010; Sigismund et al., 2005).

Upon activation by ligand binding, the EGFR becomes ubiquitinated by the E3 ligase Cbl followed by recruitment of ubiquitin (ub) binding proteins, like Eps15 and epsin, which interacts with other components in clathrin coated pits. This event leads to translocation of the EGFR into clathrin coated pits followed by invagination and pinching off from the clahtrin coated invagination (McMahon and Boucrot, 2011). Ligand bound, active and ubiquitinated receptor is sorted towards lysosomal degradation while receptors with no ligand becomes deubiquitinated and are sorted for recycling back to the plasma membrane. Internalized ligand bound receptor enters early endosomes, where ubiquitinated receptors are sorted into intraluminal vesicles (ILVs), destined for lysosomal degradation. This sorting process is controlled by the endosomal sorting complex required for sorting (ESCRT), a group of proteins located on early endosomes that recognizes ubiquitinated cargo and prevents the recycling by mediating invagination of cargo into intraluminal vesicles and in turn creating multivesicular bodies (MVBs). The ESCRT-complexes consist of four protein complexes ESCRT-0,-I,-II and -III that cooperate during the sorting of ubiquitinated cargo (Raiborg and Stenmark, 2009). The first complex, ESCRT-0, consists of a Hrs and STAM complex, which specifically binds ubiquitinated proteins and clathrin (Bache et al., 2003; Raiborg et al., 2002). Further, ESCRT-I (Katzmann et al., 2001) and ESCRT-II (Babst et al., 2002b) mediates the invagination of the membrane containing the cargo, while ESCRT-III finally pinches them off creating intraluminal vesicles (Babst et al., 2002a). During the sorting, ub is removed from cargo by deubiquitinating enzymes (DUBs), which ensure recycling of ub back to the cytoplasmic pool for new rounds of ubiquitination (Wright et al., 2011). Once sorted into ILVs, the receptor is transported towards lysosomes for degradation (Futter et al., 1996). Figure 1-4 summarizes the endocytic trafficking of the EGFR.

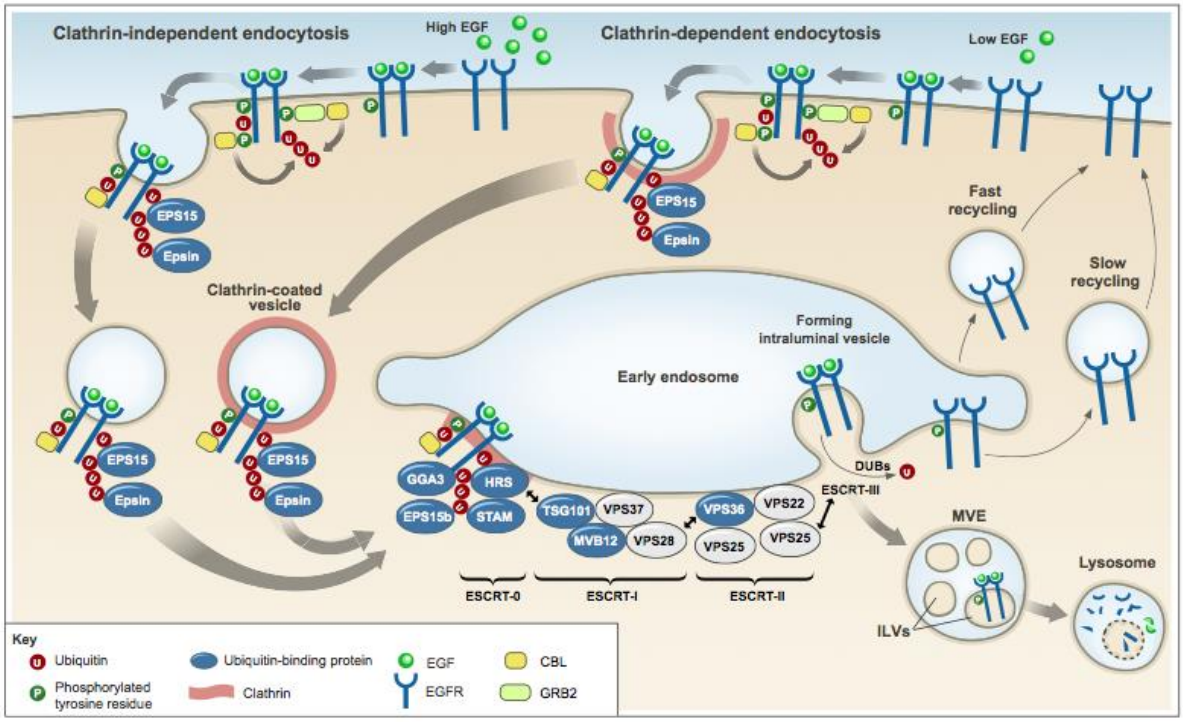

Figure 1-4. Model of EGFR endocytosis. Receptors activated by ligand binding are ubiquitinated by E3 ligases (Cbl) in order to be internalized, followed by sorting to lysosomes for degradation. High concentrations of ligand mediate clathrin-independent endocytosis while low ligand concentrations mediates clathrin- mediated endocytisis. During sorting into inner vesicles of early endosomes and MVB by the ESCRT complex, the ubiquitin molecules attached to the ligand bound receptor are removed by deubiquitinating enzymes in order to be recycled back to the cytoplasmic pool. Internalized receptors that are inactivated due to ligand dissociation are recycled back to the membrane as the cytoplasmic tail of the receptor is not ubiquitinated and thus not marked for lysosomal sorting . Figure from (Haglund and Dikic, 2012)

1.4 Ubiquitination

Ubiquitin is a 76 amino acid residue protein that can be covalently attached to other cellular proteins. Conjugation of ubiquitin (ubiqutination) is a reversible post-translational modification that may regulate the protein's localization, interaction partners, half-life and structure. In this manner, ubiquitin regulates several important cellular processes such as protein degradation, endocytic trafficking, DNA repair and transcription, autophagy, inflammation and immune responses (Woelk et al., 2007).

These ubiquitin modifications occur by covalent bonding through an isopeptide bond between the C-terminal domain on ubiquitin and the ε-aminogroup on the lysine (Lys) residue of the target protein (Goldknopf et al., 1977; Hershko et al., 1980), a step carried out by ubiquitin activating enzymes (E1), ubiquitin conjugating enzymes (E2) and ubiquitin ligases (E3) (Hershko et al., 1983). The process starts with the ATP-consuming activation of ubiquitin by the E1 enzymes, linking ubiquitin to E1 by a thioester bond, followed by transfer of the ubiquitin to the E2 enzymes by making a thioester bond. The E2 enzymes are then recruited to the E3 ligases, which recognize the target protein and finally conjugate the ubiquitin to lysines in the target substrate (figure 1-5 A). In this manner, the E3 ligase determines the type of ubiquitin modification and thus the fate of the target substrate (Husnjak and Dikic, 2012). There are two major families of E3 ligases, described below in section 1.4.1.

Ubiquitin can itself become ubiquitinated. Seven Lys residues in ubiquitin make it possible to create different kinds of modifications on the target substrate, and in this way determine the fate of the target substrate (summarized in figure 1-5 B). Essentially, ubiquitin can be attached to the substrate as one or more single moieties (mono- and multiple mono-ubiquitination) or in ubiquitin chains (polyubiquitination), where several ubiquitin moieties are covalently attached through isopeptide bonds (Husnjak and Dikic, 2012). Of these possible modifications, multiple monoubiquitination and a combination of ubiquitin chains have been under focus regarding their role in regulation of endocytic trafficking and downregulation of receptor tyrosine kinases, with EGFR as a model (Haglund et al., 2003; Huang et al., 2006; Mosesson et al., 2003).

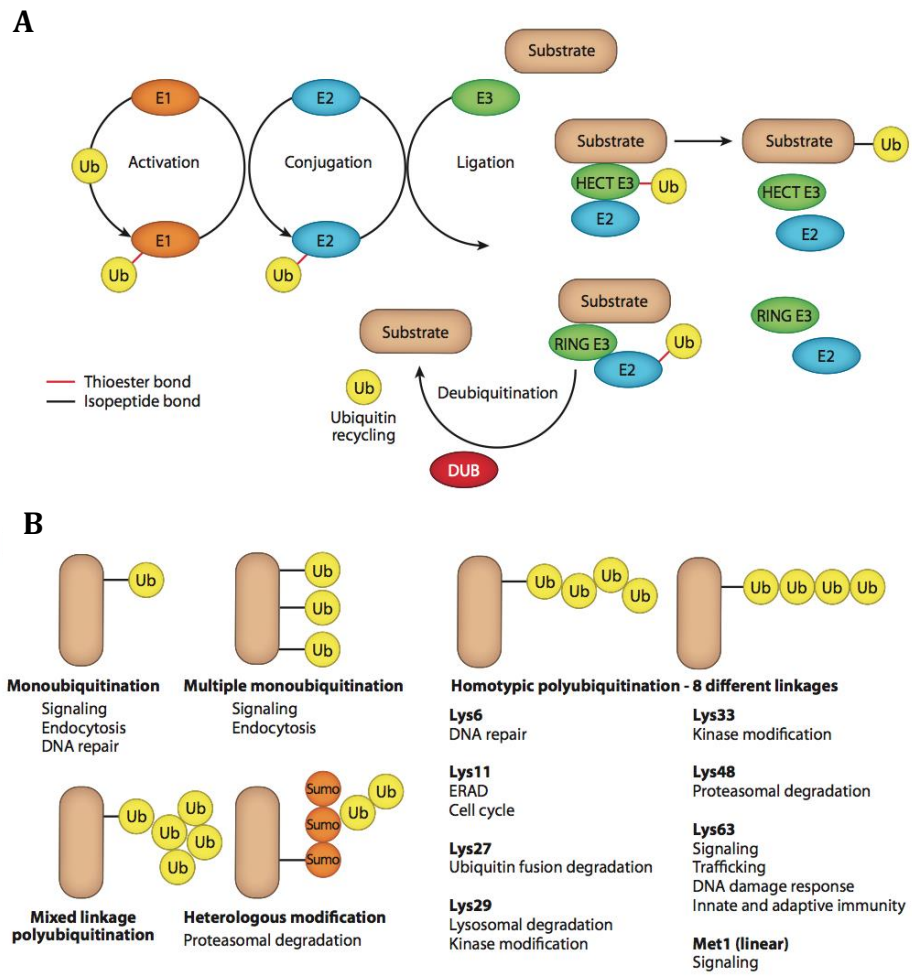

Figure 1-5. **Ubiquitin modification**. **A:** The sequential action between ubiquitin activating enzymes (E1), ubiquitin conjugating enzymes (E2) and ubiquitin ligases (E3) regulate the ubiquitination by breaking the isopeptide bond between target and ubiquitin. **B:** Various ubiquitin modifications determines the fate of the target substrate. Figure from (Husnjak and Dikic, 2012).

1.4.1 Ubiquitin ligases

As mentioned above, E3 ligases determines the fate of the substrate by identifying it as a target substrate for ubiquitination. There are two main groups of E3 ligases, RING (**r**eally-**i**ntereresting-**n**ew-**g**ene) finger E3 ligases and HECT (**h**omologous to **E**6-AP **c**arboxy **t**erminus) domain E3 ligases. The zinc-binding RING finger domain ligases mediates ubiquitination by binding the E2 and mediating the transfer of ubiquitin from E2 directly to the substrate linking ubiquitin to Lys residues in the substrate by a isopeptide bond (Freemont et al., 1991; Xie and Varshavsky, 1999), whereas for the HECT domain ligases ubiqutin is conjugated to the E3 ligase by a thioester bond before conjugating ubiquitin to Lys in the

substrate by a isopeptide bond (Huibregtse et al., 1995). DUBs regulate the level of protein ubiquitination by removing ubiquitin by cleaving of the ubiquitin-lysine isopeptide bond (Komander et al., 2009).

The RING finger E3 ligase Cbl is one of the most studied E3 ligases due to its important role as a negative regulator of various plasma membrane receptors, especially in the case of the downstream signaling of receptor tyrosine kinases like EGFR (Thien and Langdon, 2005).

1.5 The Cbl family

The Cbl proteins are evolutionary conserved RING finger E3 ligases that are ubiquitously expressed, both in mammals and non-mammals (chicken (*Gallus gallus*), zebra fish (*Danio rerio*), frog (*Zenopu tropicalis*), fly (*Drosphila melanogaster*), worm (*Caenorhabditis elegans*) and amoeba (*Dictyostelium discoideum*)) (Mohapatra et al., 2013). Dysfunction or lack of Cbl may lead to various severe disorders, such as immune diseases and cancer (Ryan et al., 2006).

c-Cbl (Cbl) was the first member to be characterized as a cellular homologue of v-Cbl, a truncated oncogenic of c-Cbl expressed in Cas-Br-M virus that induces pre-B cell lymphomas in mice. Due the oncogenic potential in the truncated form, c-Cbl was thus characterized as a proto-oncoprotein (Blake et al., 1991; Langdon et al., 1989a). Two other mammalian members were later discovered: Cbl-b (Keane et al., 1995) and Cbl-3 (Cbl-c, Cbl-SL) (Keane et al., 1999).

1.5.1 Cbl structure

The Cbl family members all have a conserved N-termini containing a tyrosine kinase binding domain (TKB) and a RING finger domain. The C-terminal domain is more divergent, which in its full length form contains proline rich regions, tyrosine phosphorylation sites and a ubiquitin associated domain (UBA) overlapping with a leucine zipper motif (LZ) (figure 1-6 A) (Huang, 2010). The TKB domain contains a four-helical bundle (4H), a calcium-binding EF domain and a SH2 domain. TKB recognizes phosphotyrosine residues on the substrate and translocates Cbl to the target protein (Meng et al., 1999). The RING finger domain serves as a binding site for the E2 ligase and is thus important for the E3 ligase activity (Joazeiro et

al., 1999). The proline rich domain and the pY residues in the C-terminal domain have binding sites for proteins containing SH3-motifs and SH2-motifs, making them important sites for interaction with adaptor- and signaling proteins. Cbl-3 has a much shorter proline-rich domain and thus interact with fewer proteins than c-Cbl and Cbl-b (Goh et al., 2010).

Once bound to the substrate, c-Cbl and Cbl-b are activated by phosphorylation of the tyrosine residues Y371 and Y363 in the linker region, respectively, by tyrosine kinases (Kassenbrock and Anderson, 2004). Both of these Cbl-isoforms have an UBA domain, but the tendency of ubiquitin binding through the UBA domain is different in c-Cbl and Cbl-b, as Cbl-b has higher ubiquitin-binding affinity than c-Cbl (Davies et al., 2004). Lastly, the LZ motifs are involved in the homodimerization of Cbl (Alber, 1992; Busch and Sassone-Corsi, 1990) (figure 1-6 B).

A

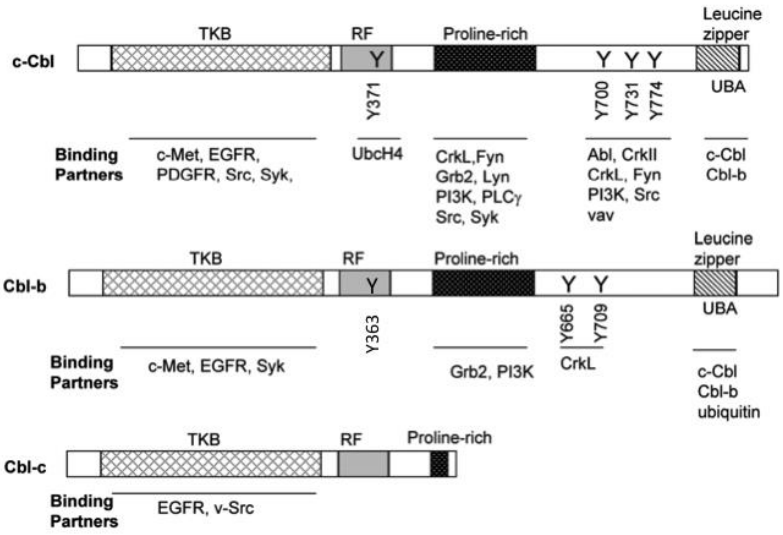

B

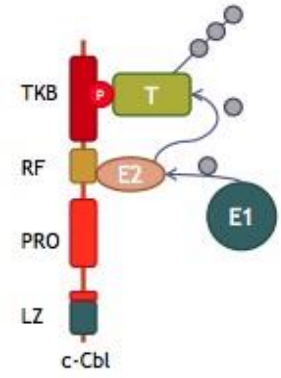

Figure 1-6. Cbl protein structure. A: The evolutionary conserved N-terminal region of the Cbl proteins contains a tyrosine kinase binding domain (TKB), a RING finger domain (RF) and a proline rich domain. The C-termimal region is more divergent and contains phosphotyrosine residues between the proline rich region and a ubiquitin associated domain (UBA) fused to a leuzine zipper domain (LZ). Modified from (Huang, 2010)**. B**: TKB recognizes and binds to phosphorylated tyrosine residues on target protein. Meanwhile, ubiquitin activating enzymes (E1) load ubiquitin and activate ubiquitin conjugating enzymes (E2). The activated E2 binds to the RING finger domain (RF) in Cbl, which further transfers ubiquitin to lysines in the target protein. Figure from Lene E. Johannessen.

1.5.2 The function and regulation of Cbl

The Cbl proteins have been extensively studied for their role in the internalization, trafficking and downregulation of the EGFR (Meisner and Czech, 1995; Yoon et al., 1995) and also in regulation of other growth factor- and immune receptors. In addition, they play an important role in regulating actin polymerization, focal adhesions and integrin through adaptor proteins that are directly involved in these processes (Huang, 2010). Since they are essential in the cell function and development, the regulation of Cbl proteins is crucial. A mechanism to control their activity is through ubiquitination of the Cbl proteins by HECT E3 enzymes, which target Cbl for proteasomal degradation (Ryan et al., 2006). It has also been proposed that lysosomes may mediate degradation of Cbl (Ettenberg et al., 2001).

1.5.3 The physiological function of c-Cbl and Cbl-b

c-Cbl is highly expressed in the thymus, serving as an important regulator for hematopoietic stem cells, and testis (Langdon et al., 1989b). It is also expressed in other organs as the spleen, lung, heart, brain as well as in T- and B cells (Huang, 2010; Rathinam et al., 2008). Like c-Cbl, Cbl-b is also expressed in hematopoietic cells, thymus, testis, heart, lung and brain. In addition, Cbl-b is expressed in the ovary, placenta, prostate, kidney, liver, skeletal muscles and especially in the spleen (Huang, 2010; Keane et al., 1995).

Mutations in c-Cbl and Cbl-b have been implicated in immune disorders, such as leukemia, due to their important role in the regulation of immune receptors in hematopoietic stem cells (Naramura et al., 2010; Rathinam et al., 2010). Other studies have shown that knockout of both c-Cbl and Cbl-b is associated with early embryonic lethality, suggesting an important role in embryonic development (Naramura et al., 2002).

The patterns of expression levels for c-Cbl and Cbl-b in different tissues also reflect the important roles for each of them. As c-Cbl is preferentially expressed in the testis and thymus, deletion of c-Cbl in germ-cells in mice has been shown to be involved in reduced male fertility (El Chami et al., 2005), increased cellular populations in lymphoid organs (Murphy et al., 1998; Rathinam et al., 2008), and alteration of positive selection of T-cells in the thymus (Naramura et al., 1998). On the other hand, Cbl-b deficient germ-cells in mice do not seem to promote abnormal developments, but rather lead to autoimmune diseases by

inducing hyperactive T-cell responses (Bachmaier et al., 2000; Chiang et al., 2000) and also a failure to induce T-cell tolerance (Jeon et al., 2004).

1.5.4 The physiological function of Cbl-3

Cbl-3 differs from c-Cbl and Cbl-b both in expression pattern, structure and physiological functions. It is mainly espressed in epithelial tissues lining the small intestine, colon, prostate, adrenal gland and salvary gland (Huang, 2010; Keane et al., 1999). Cbl-3 exhibits normal E3 ligase activity, despite its truncated structure. However, in contrast to c-Cbl and Cbl-b, Cbl-3 deficiency in mice does not seem to have any effect on the phenotype in epithelial tissues (Griffiths et al., 2003).

1.5.5 c-Cbl and Cbl-b in EGFR trafficking

c-Cbl and Cbl-b appear to have distinct roles in regulation of several receptors, especially immune receptors. c-Cbl regulates the internalization and degradation of components of T cell-receptors and B cell-receptors, while Cbl-b regulates the level of specific signaling molecules involved in T cell-receptor and B cell-receptor signaling (Badger-Brown et al., 2012; Shao et al., 2004; Thien and Langdon, 2005). Additionally, it has been reported that c-Cbl and Cbl-b has different functions in the IgE-receptor FcεRI signaling, by which Cbl-b negatively regulates mast cell degranulation significantly more than c-Cbl (Zhang et al., 2004).

However, except for some minor differences in their protein length and structure, c-Cbl and Cbl-b seems to perform the same regulatory mechanism in terms of EGFR ubiquitination and downregulation. Knockout of only one of them does not have any effect on EGFR downregulation, while knockout or downregulation of both of the Cbl´s have a significant negative effect on downregulation and internalization of the receptor (Pennock and Wang, 2008).

Upon EGFR activation, c-Cbl and Cbl-b can bind both directly and indirectly to specific phosphotyrosine residues on the receptor. Cbl can bind directly to the pY1045 site in EGFR through their SH2-domain in the TKB domain and at the same time recruit other proline rich binding proteins, like the adaptor protein Cbl-interacting protein of 85 kDa (CIN85), which is

bound through its SH3-domain to the proline rich region in Cbl. The multidomain structure of CIN85 makes it able to also interact with a variety of other proteins, which are involved several important processes such as regulation of RTK signaling, apoptotic signaling and T cell functions (Kowanetz et al., 2003; Szymkiewicz et al., 2002). Of note, CIN85 has been demonstrated to constitutively interact with the ESCRT-protein Hrs (Ronning et al., 2011). Additionally, Cbl can also bind indirectly to the pY1068 and pY1086 residues on the EGFR through the interaction of their proline rich domain with the SH3-domains in Grb2. Together, Grb2 and Cbl bind to distinct phosphotyrosine sites on the receptor and cooperate in order to mediate rapid internalization and downregulate the receptor signaling (Levkowitz et al., 1999; Waterman et al., 2002). Binding of Cbl to pY1045 is crucial for sorting of the ligand bound EGFR towards lysosomal degradation, suggested by the findings that mutation in this binding site leads to decreased degradation of receptor in lysosomes and increased recycling (Grovdal et al., 2004). On the other hand, indirect binding of Cbl to pY1068 and pY1086 is essential for internalization rather than receptor trafficking towards lysosomal degradation (Huang and Sorkin, 2005). Taken together, distinct binding patterns of Cbl to the receptor differently affects EGFR fate.

Although c-Cbl and Cbl-b appear to have overlapping functions in EGFR regulation, some differences have been reported. c-Cbl has been stated to be recruited earlier to the EGF receptor than Cbl-b, and Cbl-b seems to have prolonged association with the receptor when compared to c-Cbl. In these experiments c-Cbl appears to be strongly recruited after 15 minutes and Cbl-b after 30 min, by which Cbl-b seems to be associated with the receptor for at least 4 hours (Pennock and Wang, 2008). In addition, Pennock and Wang (2008) reported that Cbl-b may have additional binding sites in EGFR compared to c-Cbl. By using various forms of EGF receptors truncated in the C-terminal part transfected into 293T cells, Cbl-b, but not c-Cbl was found to bind truncated receptors containing amino acids 1-1044 or 1-958, lacking the identified Cbl binding site, pY1045, and the Grb2 binding sites, pY1068/1086. This suggested that Cbl-b binds to these constructs at sites not used by c-Cbl (Pennock and Wang, 2008). It has also been proposed that the UBA domain in Cbl-b can bind ubiquitinated proteins in contrast to c-Cbl. In 293T cells co-transfected with HA epitope tagged ubiquitin and c-Cbl or Cbl-b, the molecular weight of ubiquitinated proteins co-immunoprecipitated with each of the Cbls were compared. It was observed that considerable more ubiquitinated proteins with higher molecular weight was precipitated with overexpression Cbl-b, but not with c-Cbl (Davies et al., 2004). Further, c-Cbl and Cbl-b might have different roles in the

EGFR induced signaling, as overexpression of Cbl-b, but not c-Cbl, appears to inhibit the cell growth mediated by EGF-induced signaling in 32D cells overexpressing EGFR (Ettenberg et al., 1999).

Taken together, these reported differences between c-Cbl and Cbl-b in EGFR regulation give rise to further questions about their individual and cooperative functions. As different recruitment sites for Cbl in EGFR has different regulatory functions and the finding that Cbl-b may have other binding sites in EGFR when compared to c-Cbl, could indicate a more diverse regulatory function of Cbl-b compared to c-Cbl, such as in intracellular trafficking and cellular growth.

2 Aim of study

The Cbl family members c-Cbl and Cbl-b share the same functional structure and their ubiquitin ligase activity has been studied for years, of which c-Cbl has been most in focus. Nevertheles, studies on Cbl-b have shown that, in contrast to c-Cbl it is important in negative regulation of intracellular signaling leading to apoptosis and also appear to have an ubiquitin binding domain that is able to bind ubiquitinated proteins unlike c-Cbl. Even though both c-Cbl and Cbl-b are mainly expressed in the same cell types, they appear to have some different essential functions, exemplified in the importance of c-Cbl in male fertility (El Chami et al., 2005), and requirement of Cbl-b in the normal T-cell response (Bachmaier et al., 2000). Another comparative study between c-Cbl and Cbl-b proposed that Cbl-b had additional binding sites in EGFR and that they displayed different time of recruitment, by which it was demonstrated that c-Cbl was the first to bind EGFR followed by an overlap with Cbl-b that appeared to have a prolonged association with the receptor (Pennock and Wang, 2008). However, despite studies that have demonstrated differences in their functions, few other published studies have compared their activity and function in EGFR regulation.

The overall aim of this study is to look into the functions of c-Cbl and Cbl-b in EGFR regulation, by comparing their recruitment to the EGFR upon EGF stimulation and their intracellular trafficking to early endosomes.

The approach was the following:

- To study the colocalizations of c-Cbl, Cbl-b and EGF using live imaging
- To study the colocalization of c-Cbl and Cbl-b to early, Hrs-positive endosomes
- Comparison of binding of c-Cbl and Cbl-b to the EGFR by use of biochemical techniques

3 Materials and methods

3.1 Constructs

3.1.1 Plasmids and expression vectors

c-Cbl and Cbl-b were subcloned from pDsRed-momomer-C1 vector into a pcDNA3 vector containing the gene encoding the fluorescent tag mCherry by PCR-amplification of c-Cbl and Cbl-b from pDsRed-c-Cbl and pDsRed-Cbl-b, followed by restriction cutting using Not*I* and Xho*I* and ligation into the pcDNA3-mCherry vector. A schematic map over pDsRed-monomer-C1 and pcDNA3 are illustrated in figure 3-1 A and B, respectively.

A **B**

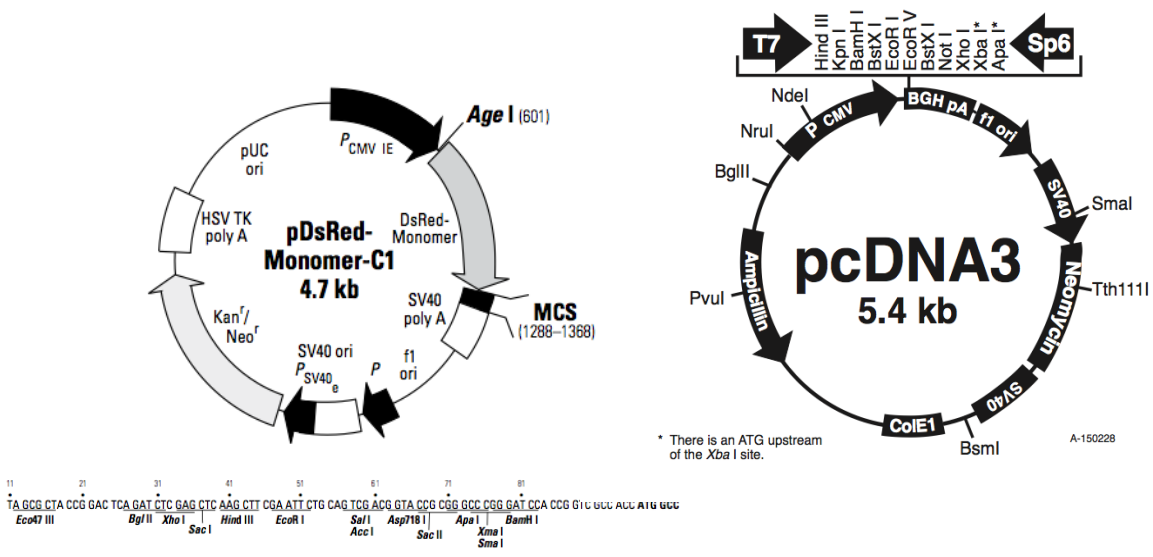

Figure 3-1. Schematic map of expression vectors pDsRed-Monomer-C1 and pcDNA3.

Other contstructs were also used in this study for both biochemical experiments and live cell imaging. An outline of the different plasmids are listed in table 3-1.

Table 3-1. List of expression contructs used in this study

Plasmid	Gene	Vector	Source
pEGFP-c-Cbl	c-Cbl	pEGFP-C1 (Clontech)	I.H. Madshus*
pcDNA3-mCherry-c-Cbl	c-Cbl	pcDNA3-mCherry (Progida et al., 2012)	Benedicte Semb Hagen
pDsRed-monomer-c-Cbl	c-Cbl	pDsRed-monomer-C1 (Clontech)	I.H. Madshus*
pEGFP-Cbl-b	Cbl-b	pEGFP-C1 (Clontech)	I.H. Madshus*
pcDNA3-mCherry-Cbl-b	Cbl-b	pcDNA3-mCherry (Progida et al., 2012)	Benedicte Semb Hagen
pDsRed-monomer-Cbl-b	Cbl-b	pDsRed-monomer-C1 (Clontech)	I.H. Madshus*
mRFP-Hrs	Hrs	mRFP (Campbell et al., 2002)	Frode M. Skjeldal**

** Inger Helene Madshus, Department of Pathology, Oslo University Hospital, Rikshospitalet, Oslo, Norway*

***Frode Miltzow Skjeldal, Department of Biosciences, University of Oslo, Oslo, Norway*

3.2 DNA techniques

3.2.1 PCR

The Cbl constructs were amplified by Polymerase Chain Reaction (PCR) of the Cbl sequence in the pDsRed-plasmid constructs using gene specific primers containing restriction sites for the restriction enzymes Not*I* and Xho*I*, which were located upstream and downstream the Cbl sequences respectively (table 3-2). Phusion High Fidelity DNA Polymerase (New England Biolabs, Ipswich, England) was used for amplification. The PCR mixture was prepared according to the enzyme manufactorer´s protocol.

Table 3-2. List of primers and restiction enzymes used in this study *

Name of primer	Tm	Primer sequence
c-Cbl forward/Not*I*	82 °C	5´ GAAGC**GGCCGC**AATGGCCGGCAACGTGAAGAA 3´
c-Cbl reverse/Xho*I*	72 °C	5´GAA**CTCGAG**CTAGGTAGCTACATGGGCAGGAGAAGAAA 3´
Cbl-b forward/Not*I*	74 °C	5´ GAAGC**GGCCGC**AATGGCAAACTCAATGAAT 3´
Cbl-b reverse/Xho*I*	66 °C	5´ GTT**CTCGAG**CTATAGATTTAGACGTGGGGATACTG 3´

*Restriction enzyme sites are written in bold

The PCR reaction programme used started with one denaturation step at 95 °C / 2 minutes, followed by 30 cycles of denaturation at 95 °C /20 seconds, annealing at 60 °C /20 seconds and amplification at 72 °C /6 minutes. The whole PCR cycle was ended by a final elongation at 72 °C /3 minutes. An overview of the PCR setup is described in table 3-3.

Table 3-3. PCR setup

Stage	Duration	Temperature (°C)	Cycles
Initial denaturation	2min	95	1
Denaturation	20s	95	30
Annealing	20s	60	
Amplification	6min	72	
Final elongation	3min	72	1

3.2.2 Agarose gel electrophoresis

DNA fragments and digested vector were separated in 1 % agarose gels. The agarose gel was prepared by dissolving 0,5 g TopVision Agarose (Thermo Scientific, Waltham, USA) and 5 µl Ethidium Bromide in 50 ml 1 x Tris-acetate-EDTA buffer (TAE, 40 mM Tris-acetate, 1 mM EDTA). 6 x sample buffer was added to the individual DNA samples before they were separated on gel using a 10K DNA ladder (Thermo Scientific, Waltham, USA) as a reference.

The agarose gel electrophoresis was performed in 1 x TAE buffer at 5 V per cm of the gel in 45 minutes. The DNA bands was detected by exposure to UV light in a UV Transilluminator (UVP, CA, USA).

DNA-fragments and digested vector were purified from the agarose gel using QIAquick Gel Extraction Kit (QIAgen, Hilden, Germany) following the manufactoter´s manual.

3.2.3 Restriction digestion and ligation of DNA fragments

The PCR products (purified from gel) and the vectors were restriction digested with the restriction enzymes Xho*I* and Not*I* with an appropriate buffer for double digestion. All enzymes and buffers were supplied by (New England Biolabs). The digestion was completed at 37 °C over night (16 hours).

The vector was run on gel and purified as described in the previous section using QIAquick Gel Extraction Kit while the digested PCR-fragments were purified with E.Z.N.A® Cycle Pure Kit (Omega Biotek, Nocross, GA, USA).

Digested c-Cbl and Cbl-b fragments were ligated into the digested pcDNA3-mCherry vector at room temperature (RT) for 2 hours utilizing 1 µl T4 DNA ligase and 1 µl 10 x T4 DNA ligase buffer (both New England Biolabs) in a final volume of 10 µl. The ratio of PCR fragment to vector was 5:1.

3.2.4 Bacterial transformation

For amplification of plasmid DNA, $CaCl_2$ competent *E.coli* Top10F cells were used for transformation. 200 µl cells were thawed on ice and incubated with 1 µg plasmid DNA on ice for 30 minutes. They were then heat shocked at 42 °C in water bath for 2 min, followed by incubation on ice for 2 minutes. 1 ml Lysogeny broth (LB) medium (prewarmed to 37 °C) was then added before incubation for 1 hour at 37 °C on a heating block. Next, the cells were pelleted by centrifugation at 4000 rpm and 90 % of the supernatant was removed before resuspension of the bacteria in the remaining solution. Transformed bacteria were then plated on an agar plate containing 100 µg/ml ampicillin or 250 µg/ml kanamycin, depending on the selection marker of the plasmid, and incbated over night in an incubator at 37 °C. Antibiotic

resistant clones were then picked and grown in 100 ml LB medium containing 100 mg/ml ampicillin or 250 mg/ml kanamycin in an incubator at 37 °C over night followed by midiprep purification.

For amplification of plasmids from a ligation mixture, XL 10-Gold Ultracompetent Cells (Agilent Technologies, CA, USA) were used for transformation. 100 µl cells were thawed and incubated on ice with 4 µl β-mercaptoethanol, included in the kit, for 10 minutes. 5 µl of the ligation mixture was added to the bacteria and they were further incubated on ice for 30 minutes. The cells were then heat shocked at 42 °C in water bath for 30 seconds followed by incubation on ice for 2 minutes. 900 µl 42 °C Super Optimal broth with Catabolite repression medium were added to the cells, and incubated in an at 37 °C incubator with shaking for 1 hour. The bacteria were then pelleted, resuspended in 200 µl LB medium and plated on agar plates containing 100 µg/ml ampicillin and incubated at 37 °C over night. pUC18 control plasmid was used as control. The ampicillin resistent clones were then grown in 1,5 ml LB medium for miniprep purification

3.2.5 Plasmid purification

E.Z.N.A.® Plasmid Mini Kit I (Omega Bio-Tek, PA, USA) and Wizard™ Plus Midipreps DNA Purification System (Promega, WI, USA) was used for small-scale and medium-scale plasmid DNA purification, respectively. Small-scale plasmid DNA was used for purification of plasmids from bacterial cells after cloning and ligation, while medium-scale plasmid DNA was used for large scale purification of plasmids. The purification was performed using the manufacturer´s manual with supplemented solutions and reagents.

3.2.6 Sequencing

Primers used for sequencing was constructed in Webprimer (http://www.yeastgenome.org/cgi-bin/web-primer) with 600 base pairs between alignment of the primers. The pcDNA3-mCherry-Cbl constructs were sequenced by GATC Biotek (Konstanz, Germany). The program CLC sequence viewer (http://www.clcbio.com/products/clc-sequence-viewer) was used for the sequence alignment.

3.3 Cell techniques

3.3.1 Cell lines and cell culture

The human epithelial cervix adenocarcinoma cell line HeLa stabily transfected with a plasmid encoding $CdCl_2$-inducable expression of invariant chain (Ii), pMEP4-Ii, (HeLa Ii) and wt HeLa cells were used in this study. HeLa cells were grown in Dulbeccos Modified Eagles Medium (DMEM) (Lonza, Basel, Switzerland) supplemented with 10 % fetal calf serum (BioSera, Boussens, France), 2 mM L-glutamine, 25 U/ml penicillin, 25 μg/ml streptomycin (all from PAA Laboratories, Pashing, Austria) and incubated in 5 % CO_2 in a 37 °C incubator. The HeLa Ii cells were grown in DMEM supplemented with 10 % fetal calf serum, 0,15 mg/ml Hygromycin B (Duchefa Biochemie BV, Haarlem, Netherlands), 2 mM L-glutamine, 25 U/ml penicillin, 25 μg/ml streptomycin and incubated in 5 % CO_2 in a 37 °C incubator. The expression of Ii was induced by incubation with 2,5 μM $CdCl_2$ over night (16-18 hours). An overview of the cell density seeded for each experiment are included in table 3-4 and 3-5.

Table 3-4. Cell density for experiments two days after seeding. HeLa (1,5 x 10^5 cells/cm^2) and HeLa Ii (4,5 x 10^5 cells/cm^2)

Cells	Dish	Area	Cells/dish	Producer	Experiment
HeLa	3,5 cm glass bottom dishes	8 cm^2	1,20 x 10^5	MatTek Corp., MA, USA	Live cell imaging
HeLa Ii	3,5 cm glass bottom dishes	8 cm^2	3,60 x 10^5	MatTek Corp., MA, USA	Live cell imaging
HeLa	6 cm	21,5 cm^2	3,22 x 10^5	Nunclon™Surface, NUNC, Roskilde, Denmark	Western blot
HeLa Ii	6 cm	21,5 cm^2	9,77 x 10^5	Nunclon™Surface, NUNC, Roskilde, Denmark	Western blot
HeLa Ii	6 well plate	9,5 cm^2	4,28 x 10^5	Nunclon™Surface, NUNC, Roskilde, Denmark	Immunoprecipitation

Table 3-5. Cell density for experiments three days after seeding. HeLa Ii (22,5 x 10^5 cells/cm^2) and HeLa (7,5 x 10^5 cells/cm^2)

Cells	Dish	Area	Cells/dish	Producer	Experiment
HeLa	3,5 cm glass bottom dishes	8 cm^2	0,6 x 10^5	MatTek Corp., MA, USA	Live cell imaging
HeLa Ii	3,5 cm glass bottom dishes	8 cm^2	1,8 x 10^5	MatTek Corp., MA, USA	Live cell imaging
HeLa	6 cm	21,5 cm^2	16,25 x 10^5	Nunclon™Surface, NUNC, Roskilde, Denmark	Western blot
HeLa Ii	6 cm	21,5 cm^2	4,85 x 10^5	Nunclon™Surface, NUNC, Roskilde, Denmark	Western blot
HeLa Ii	6 well plate	9,5 cm^2	2,14 x 10^5	Nunclon™Surface, NUNC, Roskilde, Denmark	Immunoprecipitation

3.3.2 Transient transfection

HeLa cells were seeded as described above and transfected the day before the experiment with one or two of the constructs listed in table 3-6 using Lipofectamine™ 2000 (Invitrogen, OR, USA). At the day of transfection, growth medium was removed and the cells were washed tree times with Phosphate buffered saline (PBS) before addition of DMEM w/o antibiotics, with 2 mM L-glutamine and 10 % fetal calf serum.

Lipofectamine™2000 was first mixed with Opti-MEM® (Invitrogen) and incubated for 5 minutes. In another tube, DNA was mixed with Opti-MEM®. After incubation, the Lipofectamine™2000 solution was mixed with the DNA-solution and further incubated for 20 minutes before adding the mixture to the cells. The amount of Opti-MEM®, Lipofectamine™2000 and DNA are listed in table 3-6. For cotransfections of c-Cbl and Cbl-b the two plasmids were mixed by a ratio 1:1, and for cotransfection of Hrs and either of the Cbl constructs the plasmids were similarily mixed by a ratio of 1:3.

Table 3-6. Overview of the Lipofectamine™2000 transfection mixture.

Cell culture plate	Volum of plating medium	Total DNA	Lipofectamine™	Opti-MEM®
6 well plate	2 ml	4 µg	2,25 µl	2 x 250 µl
3,5 cm dish	2 ml	2-4 µg	2,25 µl	2 x 250 µl
6 cm dish	5 ml	8 µg	3 µl	2 x 500 µl

3.4 Protein techniques

3.4.1 Cell lysis

The cells were chilled on ice and washed three times with cold PBS and lysed in cold lysis buffer (Supplementary, table S2) for 15 minutes. The lysates were then transferred to prechilled eppendorf tubes and centrifuged at 13000 x g at 4 °C for 15 minutes to remove cell nuclei and debris. The supernatant containing the proteins were transferred to new prechilled eppendorf tubes. 100 µl and 200 µl lysis buffer was used in 6 well plates and 6 cm dishes, respectively.

Cells were serum starved by incubation with DMEM (Invitrogen) supplemented with 2 mM L-glutamine, 25 U/ml penicillin, 25 µg/ml streptomycin for 4 hours before stimulation with 100 ng/ml EGF in phenol red-free HEPES-supplemented DMEM (Invitrogen) containing 25 U/ml penicillin, 25 µg/ml streptomycin and 0.1 % bovine serum albumine (Sigma Aldrich, MO, USA)

3.4.2 SDS-PAGE and Western blotting

6 x sample buffer (Supplementary, table S6) was added to the protein samples prepared for Western blot, as described above, and boiled at 95 °C in 5 minutes to denature the proteins. 20 µl of the samples were loaded on a 10 % gel (Thermo Scientific Precise™ Protein Gels, Pierce, Rockford, IL, USA) and the proteins were separated at 100 V for 70 minutes in 1 x

HEPES running buffer (Supplementary, table S3). 5 µl of the prestained standard Precision Plus Protein™ Kaleidoscope™ (Bio-Rad, Hercules, CA, USA) was used a a protein size marker.

Immobilion™ Polyvinylidene fluoride (PVDF) membranes (Millipore, Bedford, MA, USA) were pre-treated in methanol for 20 seconds, followed by incubation in dH_2O for 2 minutes and in 1 x Tris-Glycine Transfer buffer (Supplementary, table S4) for 5 minutes. The gel with the separated poteins and PVDF-membrane was assembled in an assembly cassett with the membrane facing the cathode. The separated proteins were transferred onto the PVDF-membranes at 100 V for 60 minutes at 4 °C in 1 x Tris-Glycine Transfer buffer.

The membranes were washed at room temperature for 5 minutes in Tris-buffered saline (TBS) (Supplementary, table S5) containing 0,05 % Tween®-20 (TBS-T), followed by blocking in TBS-T with 5 % blotting grade non-fat dry milk (Bio-Rad, Hercules, CA, USA) for 30 minutes. The membranes were then incubated with primary antibody diluted in TBS-T with 1% blotting grade non-fat dry milk either over night at 4 °C or for 1 hour at RT. The membranes were washed 3 x 10 times with TBS-T after incubation with primary antibody followed by blocking in 30 minutes. Further, the membranes were incubated with secondary Horseradish peroxidase (HRP)-conjugated antibody diluted in TBS-T with 1 % blotting grade non-fat dry milk either over night at 4 °C or for 1 hour at RT. Last, the membranes were washed 3 x 10 times with TBS-T and incubated in SuperSignal® West Dura Extended Duration Substrate (Thermo Scientific, Pierce, Rockford, USA) to generate a luminiscence signal. The luminescent signal was detected on Kodak Image Station 4000R (Carestream Health Inc., NY, USA) and the intensity of the bands were measured using the Carestream Molecular Imaging program (Carestream Health, Inc., NY, USA).

3.4.3 Immunoprecipitation

Magnetic Dynabeads® Protein G (Invitrogen) were used for immunoprecipitation (IP) A magnet was used to remove supernatant from the beads throughout the protocol.

50 µl of beads were used per IP. Supernatant was removed from the beads before they were incubated with 200 µl PBS containing 0,02 % Tween®-20 (PBS-T) and 1 µg of primary

antibody under rotation at RT for 60 minutes to allow the Dynabeads to bind the antibody. After incubation, the eppendorf tubes were placed on a magnet and the supernatant was removed and beads washed three times with PBS-T.

10 µl of the cell lysates were transferred to new eppendorf tubes and 2 x sample buffer (Supplementary, table S7) added to these protein samples representing the total cell lysates and boiled at 95 °C for 5 minutes to denature the proteins. The rest of the cell lysate were incubated with the antibody coupled Dynabeads from above, under rotation at 4 °C for 60 minutes.

After incubation, the Dynabeads were placed on magnet and supernatant was removed. The beads were then washed three times with 200 µl lysis buffer. Finally, the beads were resuspended in 20 µl 2 x sample buffer (Supplementary, table S7) and boiled at 95 °C for 5 minutes before being loaded onto SDS-PAGE-gels and analyzed by Western Blotting as described above.

3.4.4 Antibodies

All antibodies used in this study are listed in supplementary, table S1**.**

3.5 Imaging techniques

HeLa and HeLa Ii cells were seeded on 3,5 cm glass bottom dishes and left to adhere for 24 or 72 hours before being transiently transfected with DNA of interest using Lipofectamine™2000, as previously described. At the day of the live imaging experiment, the cells were washed 3 times with 1 x PBS prewarmed to 37 °C before adding phenol red free, HEPES-supplemented DMEM containing 10 % fetal calf serum. EGF conjugated with Alexa 647 (Invitrogen) was added to cells under the microscope while imaging (final concentration 100 ng/ml), in order to initiate activation and internalization of the EGF receptor. The cells were maintained inside a 37 °C chamber during the imaging.

The live cell imaging was carried out using PlanApo 60x/1,42 oil objective on an Olympus IX-71 microscope (Olympus, Hamburg, Germany), set up with a CSU22 Spinning Disk confocal unit (Yokogawa, Tokyo, Japan) and an iXonEM+EMCCD camera (Andor, Belfast, UK). The fluorochromes were excited with an Argon laser emitting 488 nm, 559 nm or 647 nm. All live imaging experiments were excecuted with one frame per 5 or15 seconds for 12-87 minutes, and the images were prepared using Andor iQ 1.8.1 software and ImageJ (NIH, Bethesda, MD).

3.5.1 Image analysis

The images were analysed in ImageJ. The area around the cell was subtracted to give the region of interest (ROI). The area in ROI was subjected to background subtraction using the built-in rolling-ball algorithm. The images were thresholded so the structures positive for Cbl, EGF or Hrs could be detected and the number of pixels representing the structures were quantified.

The colocalizations were analysed using the colocalization plug-in, which superimposes the pixels from the two respective thresholded images and quantifies the number of colocalized pixels in the ROI. Subsequently, the number of pixels showing colocalization was expressed as a proportion of the total thresholded pixels for each of the given proteins, by dividing the number of pixels showing colocalization by the number of thresholded pixels for each of the individual channels at each time point.

4 Results

4.1 Construct design and characterization of cell lines

In order to optimize the visualization of red fluorescence protein tagged c-Cbl and Cbl-b under live imaging, c-Cbl and Cbl-b were cloned into the pcDNA3-mCherry vector as mCherry is a more photostable and brighter protein than DsRed (Shaner et al., 2005). First, a gene encoding Rab7b originally included in pcDNA3-mCherry was removed by restriction digestion using Not*I* and Xho*I*. PCR-amplified Cbl-sequences were digested using the same restriction enzymes (Not*I* and Xho*I*) and subcloned into the digested pcDNA3-mCherry construct, downstream of the mCherry gene and cytomegalovirus (CMV) promoter (figure 4-1).

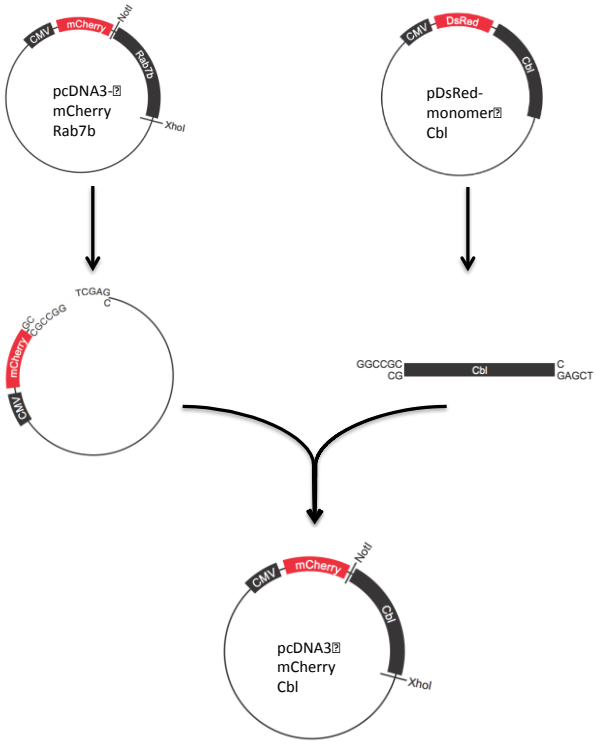

Figure 4-1: **Illustration of the subcloning of the Cbl-gene from pDsRed-monomer-C1 into pcDNA3-mCherry.** The gene encoding Rab7b was removed from the pcDNA3-mCherry-Rab7b plasmid by restriction digestion using the enzymes Not*I* and Xho*I*. The Cbl-sequences were amplified by PCR using primers containing the same restriction sites as used for pcDNA3-mCherry-Rab7b. The amplified Cbl-sequences were cut by Not*I* and Xho*I* and ligated into the pcDNA3-mCherry vector.

To identify plasmids containing the correct Cbl-insert, several clones of the pcDNA3-mCherry-Cbl constructs were digested with Not*I* and Xho*I*, as described in section 3.2.3. The digestion reactions were loaded on a 1% agarose gel to identify plasmids containing the Cbl insert (figure 4-2 A and B). Several of the plasmids showed a band of correct sizes, around 3000 base pairs, representing the Cbl insert. The plasmids displaying correct band sizes were verified by sequencing, as described in section 3.2.6. To verify that expression of mCherry-c-Cbl and mCherry-Cbl-b were induced properly from the mCherry-plasmids, HeLa Ii cells were transiently transfected with pcDNA3-mCherry-c-Cbl or pcDNA3-mCherry-Cbl-b before lysis and blotting against antibodies specific for c-Cbl and Cbl-b (figure 4-2 C and D). Non-transfected HeLa Ii cells expressing only endogenous c-Cbl and Cbl-b were used as negative control, while HeLa Ii cells transfected with EGFP-Cbl or DsRed-Cbl were used as a positive control. The cells transfected with mCherry-Cbl showed bands at similar size as for the positive controls, indicating that the constructs were correctly expressed in the cells.

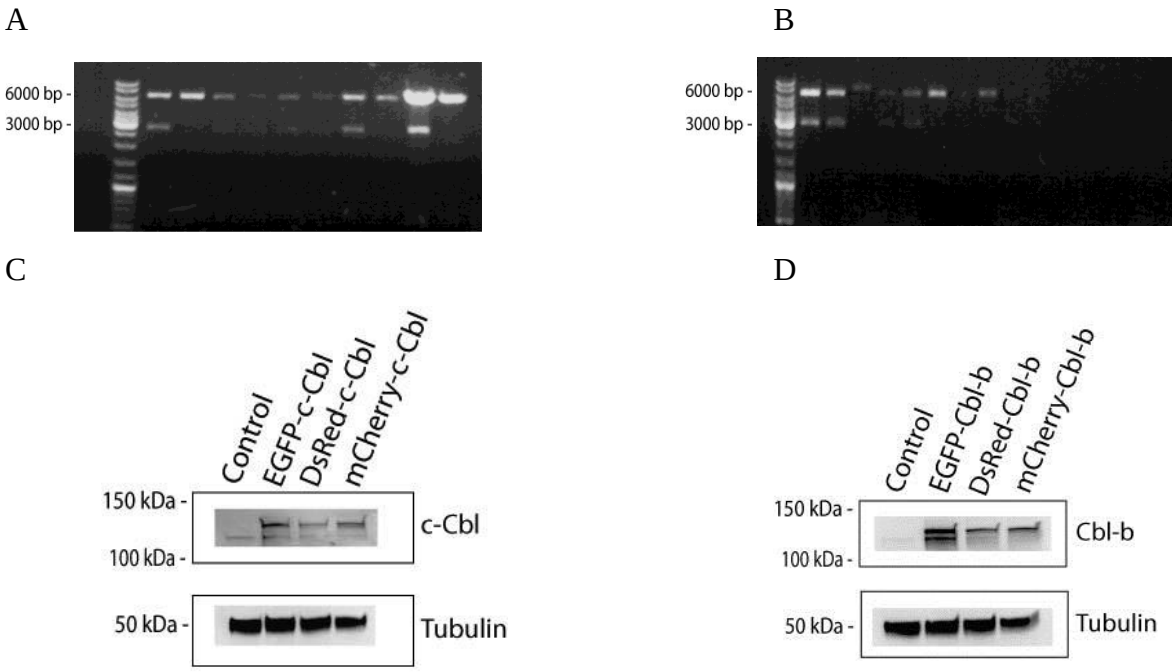

Figure 4-2: Verification of plasmids expressing mCherry-Cbl. A and **B:** Identification of plasmids containing the Cbl insert. Several different clones of pcDNA3-mCherry-c-Cbl (**A)** and pcDNA3-mCherry-Cbl-b (**B)** were digested with Not*I* and Xho*I* in appropriate buffers at 37 °C over night. 6 x sample buffer was added to the digested plasmids before being loaded onto a 1 % agarose gel. A band of approximately 3000 bp, the correct size of the Cbl-inserts, could be detected in several clones. **C** and **D:** Expression of mCherry-Cbl in Hela Ii cells. HeLa Ii cells were transiently transfected with pcDNA3-mCherry-Cbl-plasmids, using pEGFP-Cbl- and

pDsRed-Cbl constructs as positive controls. Non-transfected cells were used as a negative control. The cells were lysed and the proteins were separated on SDS-PAGE. The proteins were transferred to a PVDF membrane blotted with antibodies specific for c-Cbl and Cbl-b, respectively. The membranes were blotted with an antibody against Tubulin as loading control. Expression of both mCherry-c-Cbl (**C)** and mCherry-Cbl-b ccould be detected **(D)**.

4.1.1 Imaging of mCherry-Cbl

As a final control, HeLa Ii cells transfected with mCherry-c-Cbl or mCherry-Cbl-b were analyzed under confocal microscope. Unfortunately, the expression of the mCherry-Cbl constructs appeared to cause aggregation of the mCherry-Cbl proteins in the majority of the transfected cells (figure 4-3 A and B) and the mCherry constructs did not translocate to the EGFR upon EGF addition (confocal imaging, data not shown). For this reason, DsRed was utilized as red fluorescent tag for Cbl in further experiments.

A **B**

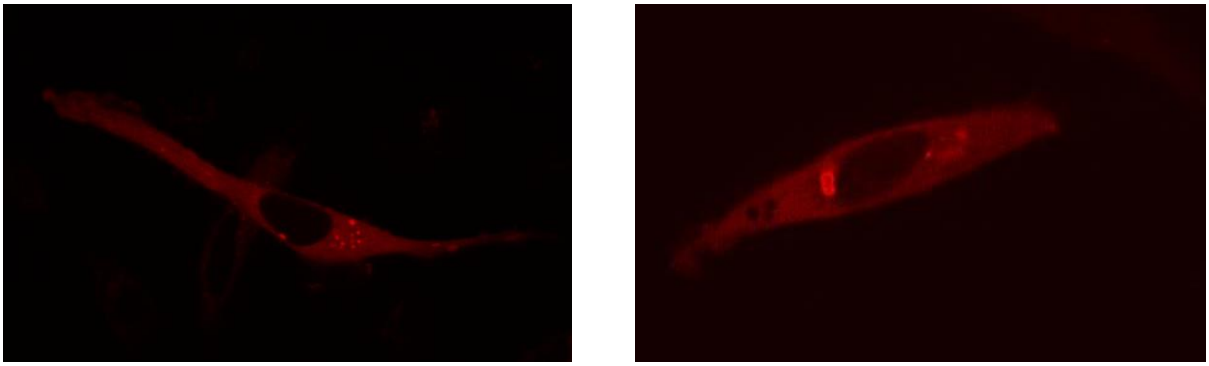

Figure 4-3. Confocal microscopy of mCherry-Cbl. HeLa Ii cells seeded onto 3,5 cm dishes and transiently transfected with either mCherry-c-Cbl (**A)** or mCherry-Cbl-b (**B)** over night. The cells were imaged at 37 °C using a Spinning Disc confocal microscope with lasers emitting fluorescent light at 555 nm wavelength.

4.1.2 Cell lines

HeLa Ii were initially intended to be used for live imaging due to their ability to express Ii through its $CdCl_2$ inducable promoter. Ii expression induces formation of enlarged endosomes, which makes it easier to visualize different domains on endosomes and therefore if two proteins on the same endosome actually colocalize on the same endosomal domains. However very few cells containing Ii induced enlarged endosomes expressed the transfected

Cbl constructs. In most of the cells expressing the Cbl-constructs, enlarged endosomes could not be detected. Additionally, Hela Ii cells with induced enlarged vesicles appeared to be particularly sensitive towards live imaging. For this reason, wt HeLa cells were also used in the following experiments. Both HeLa Ii and HeLa cells express EGFR, c-Cbl, Cbl-b and Hrs endogenously (figure 4-4).

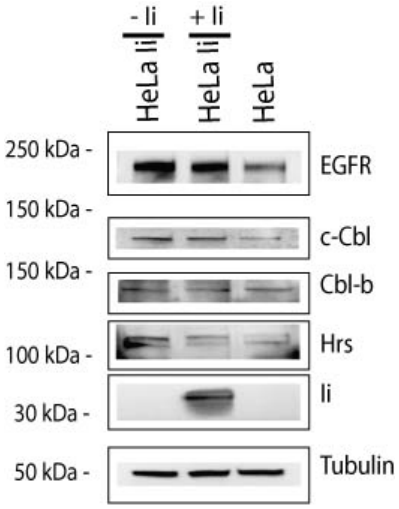

Figure 4-4: Endogenous expression of EGF receptor, c-Cbl, Cbl-b and Hrs in HeLa Ii and HeLa cells.
HeLa Ii (without or with Ii induction) and HeLa cells were lysed and the proteins were separated on SDS-PAGE. The proteins were transferred onto a PVDF membrane and blotted with antibodies specific for EGFR, c-Cbl, Cbl-b, Hrs, and Ii. The membranes were blotted with an antibody against Tubulin as a loading control.

4.2 c-Cbl and Cbl-b show similar colocalization characteristics with EGF

To investigate the trafficking of c-Cbl and Cbl-b towards activated EGFR, HeLa cells were transiently cotransfected with DsRed-c-Cbl and EGFP-Cbl-b and imaged under a Spinning Disc confocal microscope. Hela cells endogenously expressing EGFR were stimulated with 100 ng/ml Alexa 647-tagged EGF. EGFR ligand addition induced a distinct recruitment of DsRed-c-Cbl and EGFP-Cbl-b to EGF, at which it was much easier to detect Cbl-b regardless of the tag used, suggesting that there could be a stronger recruitment of Cbl-b than c-Cbl to the EGFR (figure 4-5, movie S1 and data not shown). However, despite the weaker signal from DsRed-c-Cbl on EGF positive endosomes, we could observe a similar recruitment pattern of c-Cbl and Cbl-b.

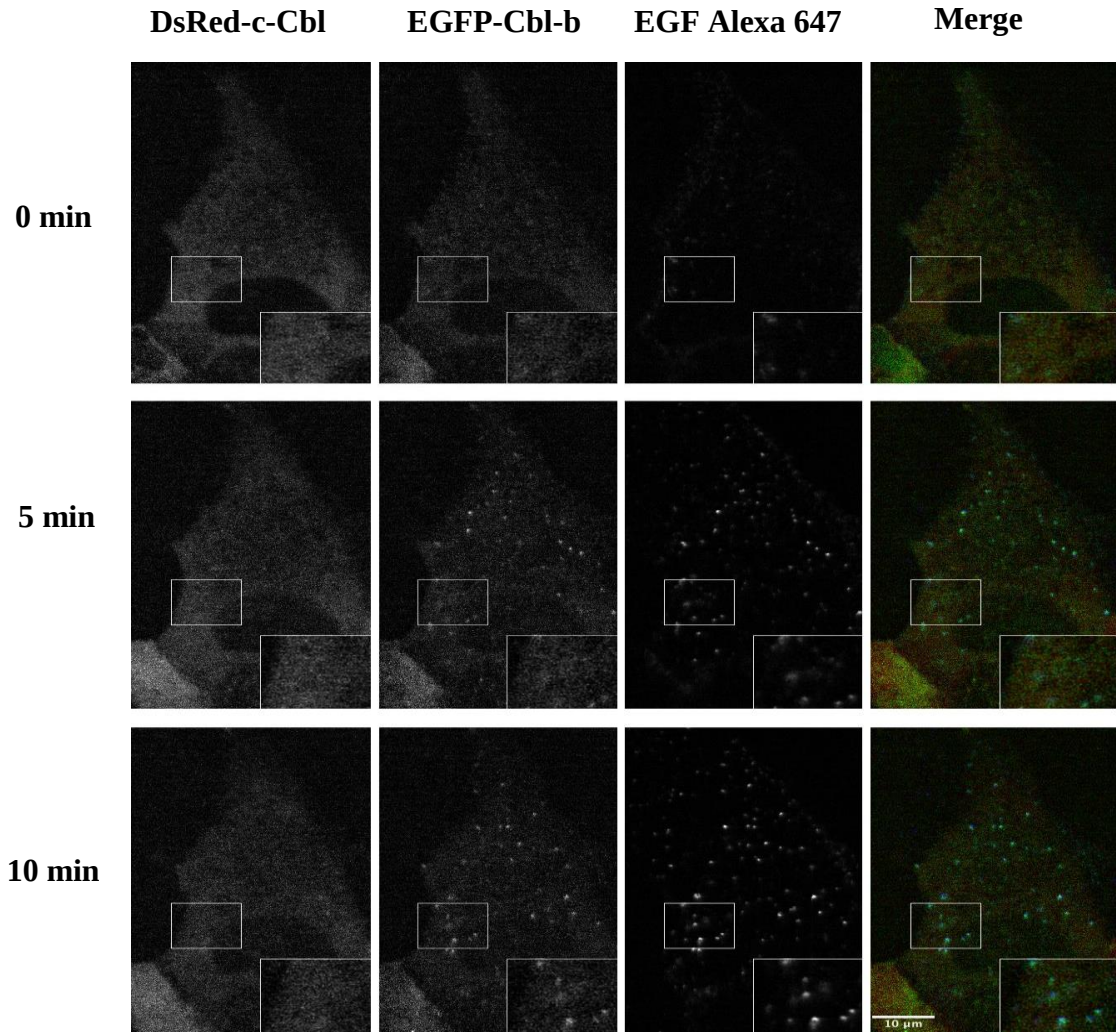

Figure 4-5: Trafficking of c-Cbl and Cbl-b with EGF. HeLa cells were transiently cotransfected with DsRed-c-Cbl and EGFP-Cbl-b and stimulated with 100 ng/ml Alexa 647-tagged EGF under live imaging at 37 °C using Spinning Disc confocal microscopy with lasers emitting fluorescent light at 488, 555 nm and 647 wavelength.

The pixels representing c-Cbl, Cbl-b and EGF structures were analyzed, and the amount of the given proteins in the colocalized area was further quantified as described in section 3.5.1. The quantifications showed that when measuring the total number of colocalized pixels in the cell, colocalization of c-Cbl and Cbl-b with EGF both started after around 3 minutes, followed by a plateu (figure 4-6 A and C). However, the weak signal from DsRed-tagged c-Cbl lead to high pixel background and therefore less certainty regarding c-Cbl measurements. When quantifying the fraction of each protein that colocalized with an other protein, based on number of pixels (figure 4-6 B and D), an increased proportion of pixels representing c-Cbl

on EGF structures could be detected over time, coinciding with increased recruitment to EGFR. However, it was difficult to establish the pattern due to the weak signal from c-Cbl. An increased proportion of pixels representing Cbl-b on EGF structures could be detected at early time points followed by a plateu, which was as expected when compared to the plateu in figure C. The proportion of EGF colocalizing with c-Cbl or Cbl-b over time was low. This could be due to a much larger size of the EGF structures than the Cbl-stuctures, which would lead to more EGF pixels than Cbl pixels on what that supposedly is the same endocytic vesicle. Another explanation could be saturation of the cell with Alexa 647-tagged EGF during stimulation, which might lead to alternative endocytic pathways.

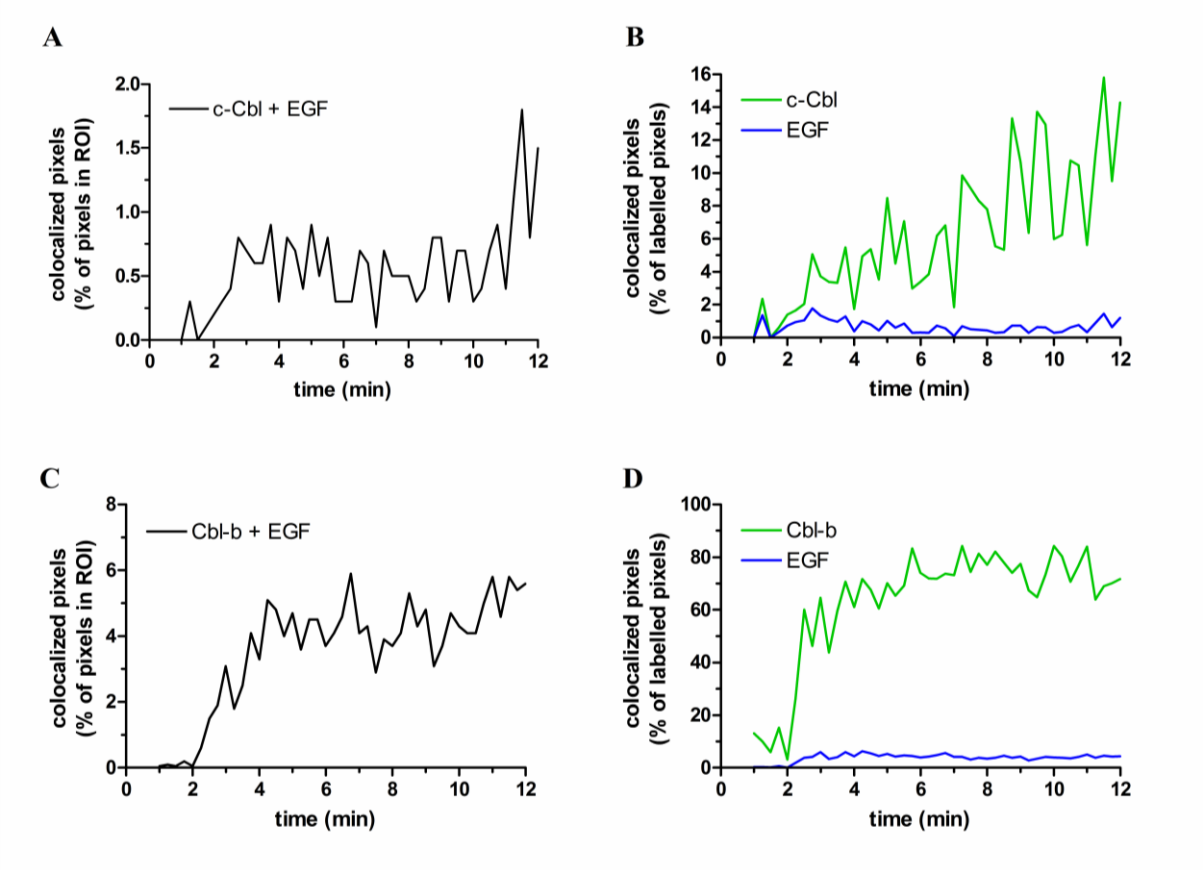

Figure 4-6: Quantification of colocalization of c-Cbl and EGF, and Cbl-b and EGF. Quantification of live imaging in figure 5-5 (movie S1), analyzed in ImageJ.

A and C: Percentage of colocalized pixels measured as number of pixels showing colocalization of c-Cbl and EGF (**A)** or Cbl-b and EGF (**C)** out of total number of pixels in ROI. **B and D**: Percentage colocalization measured as fraction of colocalized pixels relative to the total number of c-Cbl or EGF pixels (**B)** or number of Cbl-b or EGF (**D)** pixels in the ROI. The analysis was based on one experiment.

4.3 Binding of c-Cbl and Cbl-b to EGFR show a different efficiency of recruitment

The previous imaging experiment could indicate that although both Cbls seem to localize together with EGF on endosomes at the same time points, Cbl-b was recruited more efficiently to the EGFR than c-Cbl, as the Cbl-b-structures were rapidly detected and gave a stronger signal than c-Cbl. To address this further, we investigated the recruitment of Cbl to EGFR upon EGFR activation by IP studies. In this experiment, HeLa Ii cells without Ii induction were transiently transfected with EGFP-c-Cbl or EGFP-Cbl-b and stimulated with EGF for the indicated time points. The time courses of the shown experiments were limited to 12 minutes, since it has previously been demonstrated that expression of Cbl leads to EGF receptor induced phosphorylation of Hrs within this period of time (Stern et al., 2007). Non-stimulated cells were used as a negative control and stimulation for 60 min on ice as positive control to detect the total amount of c-Cbl and Cbl-b recruited to EGFR at the PM. EGFP-c-Cbl and EGFP-Cbl-b were immunoprecipitated using antibody against GFP, and the immunoprecipitated proteins were further analyzed by Western blotting using antibodies specific for EGFR and GFP (figure 4-7 A). The intensity of the EGFR bands relative to the Cbl-bands were further quantified (figure 4-7 B). A higher proportion of EGFR was precipitated with Cbl-b over time than with c-Cbl, in accordance with the previous imaging experiment. Except for the more efficient recruitment of Cbl-b than c-Cbl to the EGFR, the tendency of the time courses were the same, also coinciding with the previous imaging experiment.

A

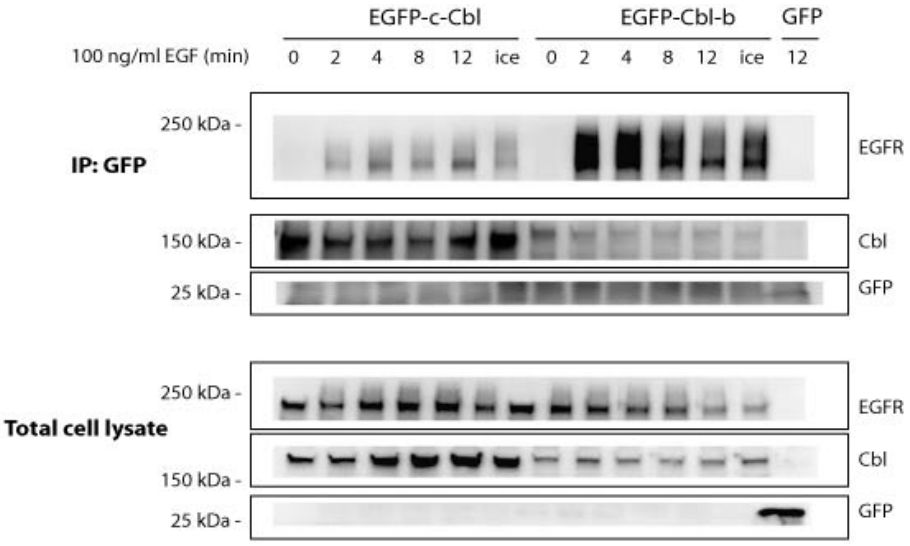

B

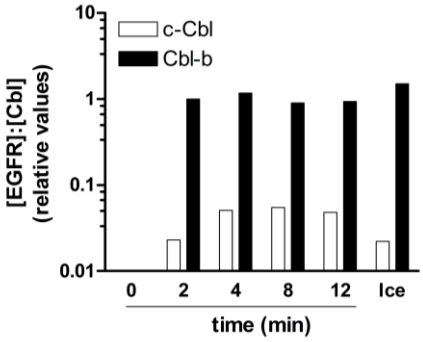

Figure 4-7: Recruitment of Cbl to EGFR. A: HeLa Ii cells were transiently transfected with either EGFP-c-Cbl or EGFP-Cbl-b and stimulated with 100 ng/ml EGF for the indicated time points. The cells were lysed and immunoprecipitated with antibody against GFP. The samples were further blotted with antibodies specific for EGFR and GFP (Cbl and GFP). **B:** The intensities of the immunoreactive bands in **A** were analyzed in Carestream M1. The EGFR:Cbl ratios were calculated and normalized to the EGFR:Cbl-b value at 2 min for easier comparison. The data represents one representative out of four independent experiments showing similar results.

4.4 c-Cbl and Cbl-b colocalize with Hrs at similar time points

Cbl has been reported to increase EGFR induced phosphorylation of Hrs, and this phosphorylation seems to be an important mechanism for correct trafficking of EGFR to lysosomes (Stern et al., 2007). After observing the more efficient recruitment of Cbl-b to EGFR when compared to c-Cbl, we further wanted to study if these differences could influence the trafficking of EGFR to Hrs positive endosomes. The trafficking was studied by transient cotransfections with either EGFP-c-Cbl and RFP-Hrs or EGFP-Cbl-b and RFP-Hrs.

4.4.1 c-Cbl and Hrs

In the experiment for c-Cbl, HeLa cells were transiently cotransfected with EGFP-c-Cbl and RFP-Hrs and stimulated with Alexa 647-tagged EGF under live imaging. Stimulation of EGFR with EGF showed a rapid recruitment of c-Cbl to EGF structures and they appeared to colocalize during internalization and intracellular trafficking (figure 4-8, movie S2).

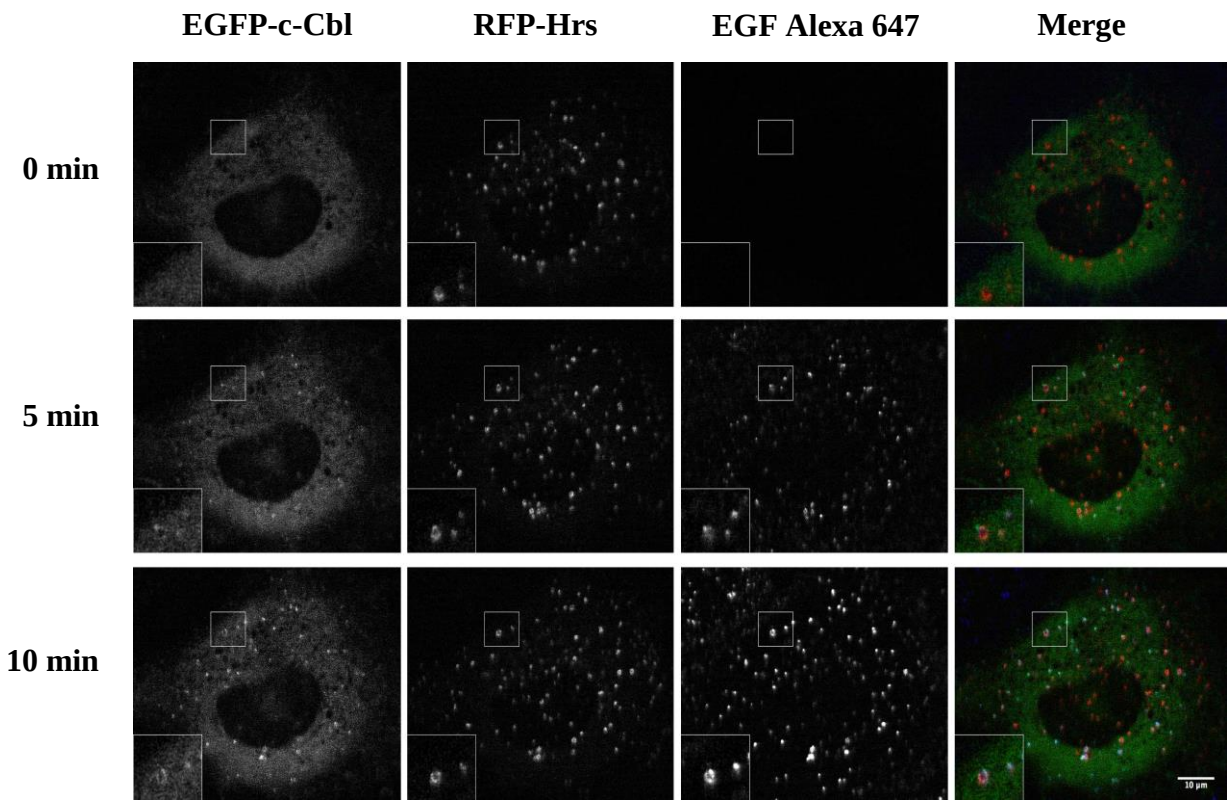

Figure 4-8: Trafficking of c-Cbl to Hrs-positive vesicles after EGF stimulation. HeLa cells were transiently cotransfected with EGFP-c-Cbl and RFP-Hrs at 37 °C over night and stimulated with 100 ng/ml Alexa 647–tagged EGF under live imaging using Spinning Disc confocal microscopy with lasers emitting fluorescent light at 488, 555 nm and 647 wavelength.

We further analyzed colocalization over time for c-Cbl and EGF, c-Cbl and Hrs, and Hrs and EGF to better get a picture of the trafficking pattern. These data showed that colocalization of c-Cbl and EGF could be detected after 4 minutes (figure 4-9 A), indicating a rapid recruitment to EGF and correlating with the findings in c-Cbl and Cbl-b cotransfected cells (figure 4-6). Analyzing the proportion of c-Cbl involved in colocalization with EGF revealed that by 10 minutes after stimulation, there seems to be a plateu of the thresholded c-Cbl signal colocalizing with EGF (figure 4-9 B). Analysis of c-Cbl and Hrs demonstrated that the colocalization started around 4 minutes, at which there was a steady increase in the number of pixels representing c-Cbl that colocalized with Hrs (figure 5-9 C and D). Lastly, colocalization of Hrs and EGF appeared to start after 4 minutes, where there was a high proportion of pixels respresenting EGF colocalization with Hrs, suggesting a rapid trafficking pattern of EGFR to Hrs-positive early endosomes (figure 5-9 E and F).

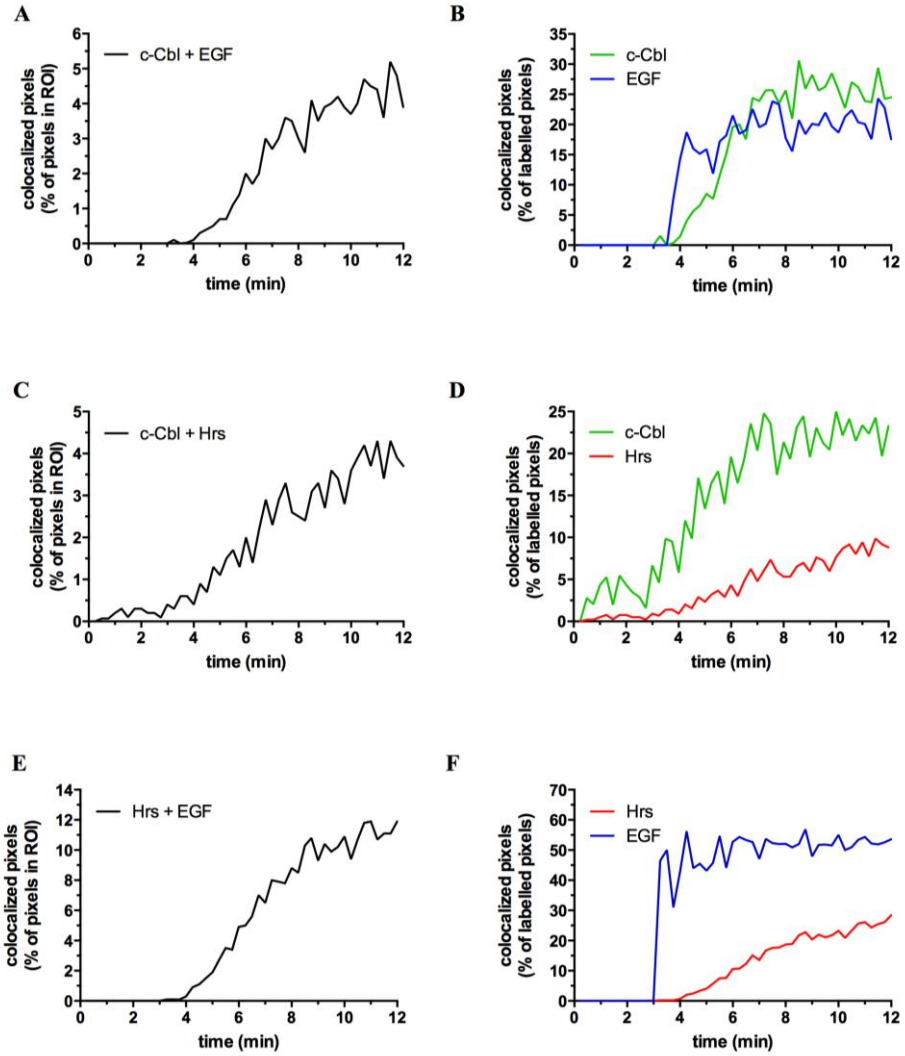

Figure 4-9: Colocalization of c-Cbl and EGF, c-Cbl and Hrs and Hrs and EGF. Quantification of live imaging in figure 4-8 (movie S2), analyzed in ImageJ.

A: Percentage colocalization of c-Cbl and EGF in ROI. **B:** Percentage colocalization relative to the amount of c-Cbl or EGF in the ROI. **C:** Percentage colocalization of c-Cbl and Hrs in ROI. **D:** Percentage colocalization relative to the amount of c-Cbl or Hrs in the ROI. **E:** Percentage colocalization of Hrs and EGF in ROI. **F:** Percentage colocalization relative to the amount of Hrs or EGF in the ROI.

4.4.2 Cbl-b and Hrs

For experiments with Cbl-b, HeLa Ii cells with Ii induced enlarged endosomes were transiently cotransfected with EGFP-Cbl-b and RFP-Hrs and stimulated with Alexa 647 – tagged EGF under live imaging (figure 4-10, movie S3).

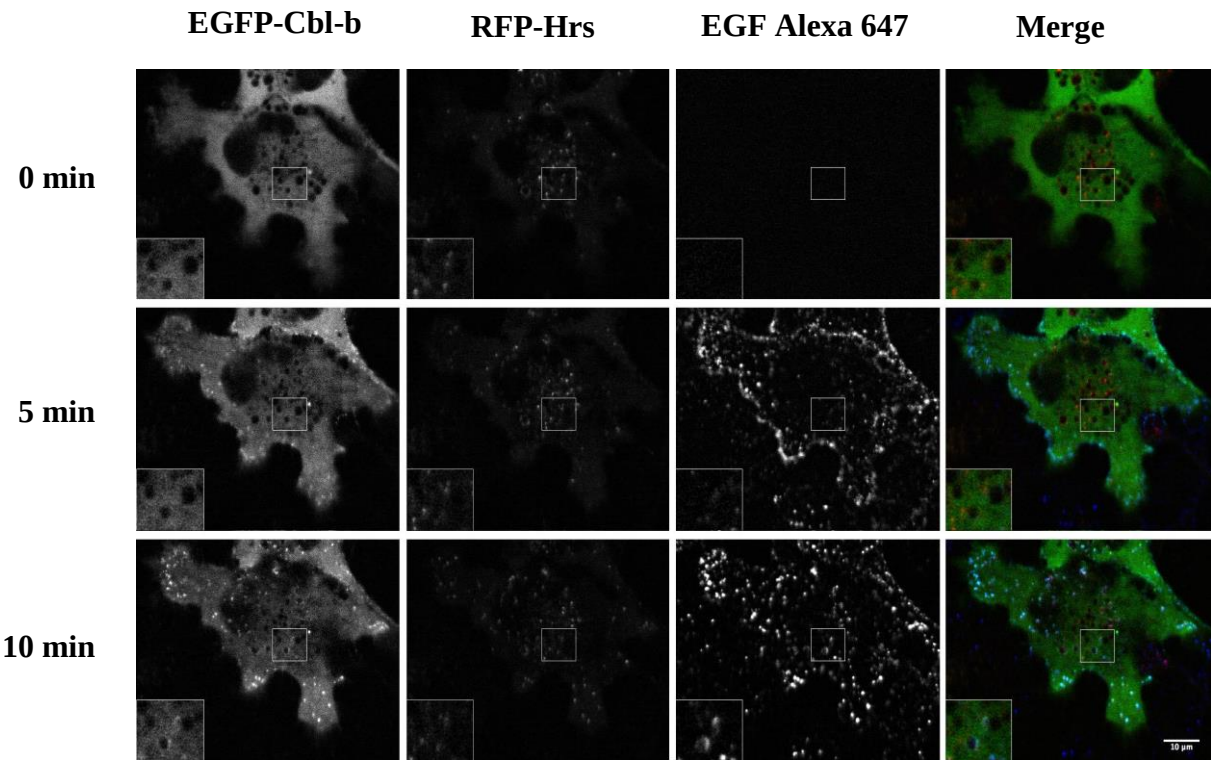

Figure 4-10. The number of Cbl-b- and Hrs positive vesicles after EGF stimulation. HeLa Ii cells were transiently cotransfected with EGFP-Cbl-b and RFP-Hrs at 37 °C over night and stimulated with 100 ng/ml Alexa 647-tagged EGF under live imaging using Spinning Disc confocal microscopy with lasers emitting fluorescent light at 488, 555 nm and 647 wavelength.

Further analysis showed that the colocalization of Cbl-b and EGF could be detected after 2 minutes (figure 4-11 A), comparable to the findings in c-Cbl and Cbl-b cotransfected cells (figure 4-6). Further quantifications showed a rapid increase in the amount of Cbl-b pixels colocalizing with EGF pixels, also correlating with the observations in cells cotransfected with c-Cbl and Cbl-b. The small drop in the amount of Cbl-b that colocalized with EGF after 4-5 min was not observed in the cells cotransfected with c-Cbl and Cbl-b and might simply be due to cell-to-cell variation, as quantifications are based on one cell only. Further, the

amount of EGF colocalizing with Cbl-b positive structures seemed to increase throughout the time course (figure 4-11 B). Colocalization of Cbl-b and Hrs showed a steady increase after 4 minutes (figure 4-11 C), correlating with cells cotransfected with c-Cbl and Hrs (figure 4-9 C). Analyzing the proportions of Cbl-b and Hrs colocalizing with each other revealed a similar time course pattern for both proteins (4-11 D). Lastly, Hrs and EGF showed colocalization after 4 minutes (figure 4-11 E), which is similar to c-Cbl in cells cotransfected with c-Cbl and Hrs (figure 4-9 E). Further, the analysis showed that there was a steady increase in the number of pixels showing colocalization of EGF and Hrs, suggesting a gradual trafficking of EGFR to early endosomes (figure 4-11 F).

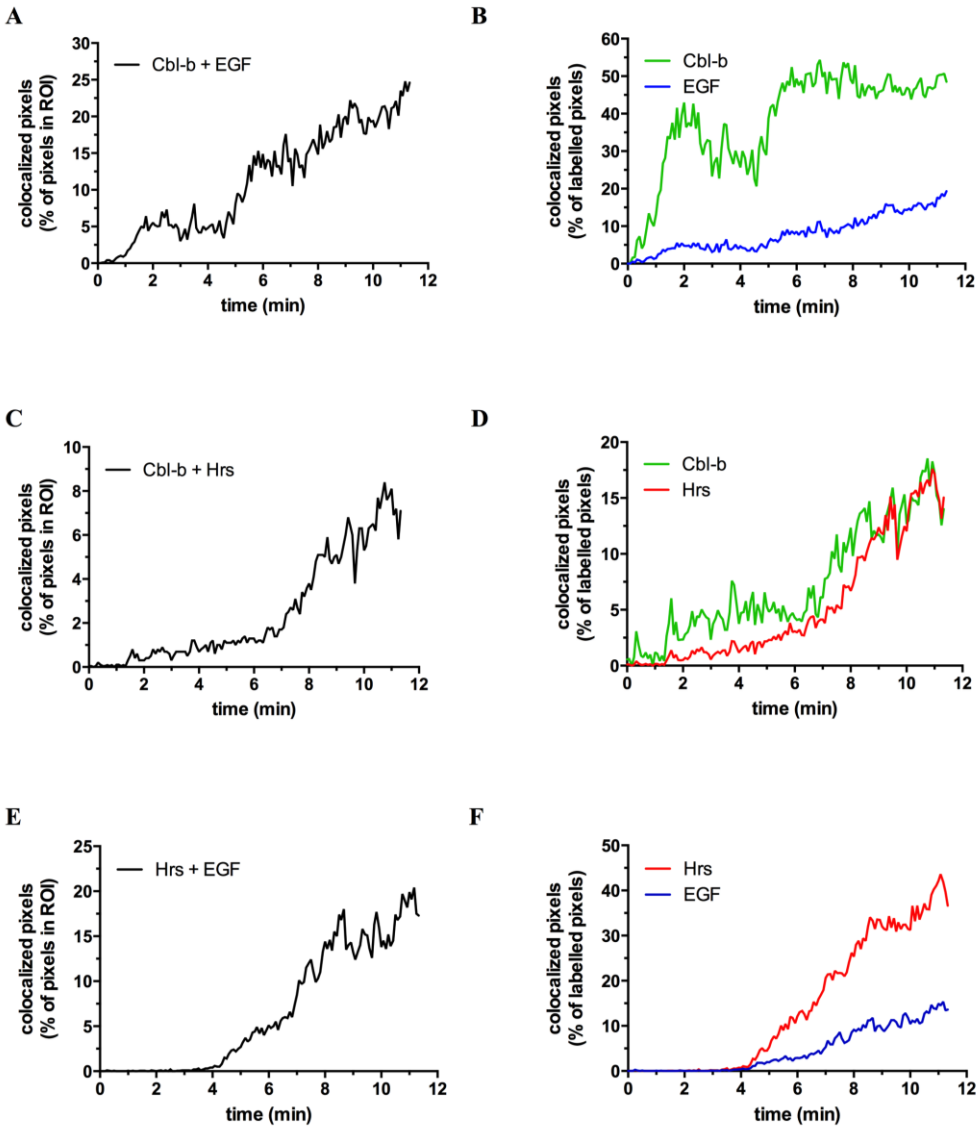

Figure 4-11: Quantification of colocalization of Cbl-b and EGF, Cbl-b and Hrs and Hrs and EGF.
The images from live imaging in figure 4-10 (movie S3) were analyzed in ImageJ.

A: Percentage colocalization of c-Cbl and EGF in ROI. **B:** Percentage colocalization relative to the amount of c-Cbl or EGF in the ROI. **C:** Percentage colocalization of c-Cbl and Hrs in ROI. **D:** Percentage colocalization relative to the amount of c-Cbl or Hrs in the ROI. **E:** Percentage colocalization of Hrs and EGF in ROI. **F:** Percentage colocalization relative to the amount of Hrs or EGF in the ROI.

5 Discussion

In this thesis I have investigated whether the two isoforms of the ubiqutin ligase Cbl, namely c-Cbl and Cbl-b, differently affect EGFR trafficking at early time points. c-Cbl and Cbl-b have been thought to have the same and overlapping function in the internalization and intracellular trafficking of activated EGFR. However some difference have been reported. Of note, c-Cbl seems to be recruited earlier to the receptor than Cbl-b and Cbl-b appears to have prolonged association with the receptor (Pennock and Wang, 2008). Further, Pennock and Wang (2008) proposed that Cbl-b has additional binding sites in the phosphorylated receptor compared to c-Cbl. Also, Cbl-b has been shown to regulate cellular growth through EGFR signaling to a larger extent than c-Cbl (Ettenberg et al., 1999). Taken together, even though c-Cbl and Cbl-b display similar regulatory functions in EGFR internalization and trafficking, questions still remain about their individual functions.

As Cbl proteins are essential for correct EGFR internalization and degradation following activation, we wanted to investigate whether any differences could be detected between c-Cbl and Cbl-b in EGFR trafficking by studying the recruitment of c-Cbl and Cbl-b to the activated EGFR and their trafficking to early endosomes. In order to investigate this, both biochemical assays and live imaging were conducted. HeLa Ii cells were initially selected for the experiments due to their ability to induce expression of Ii by addition of $CdCl_2$, which in turn induces enlarged endosome. Hela Ii cells without induction of Ii were chosen for biochemical analysis, while Hela Ii cells with induced Ii-expression were chosen for live imaging, in order to avoid clonal differences. Endosomes contain many separate domains and two proteins on the same endosome might be localized to different microdomains. The Ii enlarged endosomes would make it easier to detect any possible colocations between two proteins on the same endosome by live imaging. However, there were several problems regarding the transient transfections and induction of expression of Ii. Wt HeLa cells were therefore also used and is the reason for different cell lines in the experiments. HeLa Ii cells appeared not display any different pattern of EGF endocytosis compared to HeLa (Supplementary, figure S1). The differences at early time points might be due to variations in EGFR expressions and thus different amount of EGF binding to the cells, which would result in differences in amount of pixels representing EGF structures. However, it seems that the pattern of internalization is essentially the same, as the curved appears to have the same peak.

Also, expression of endogenous Cbl-proteins and EGFR was the same in both cell lines (figure 4-4)

To investigate the intracellular trafficking of c-Cbl and Cbl-b, HeLa cells were transiently cotransfected with DsRed-c-Cbl and EGFP-Cbl-b, and EGFR was stimulated with Alexa 647-labeled EGF (figure 4-5). The analysis from live imaging showed that both c-Cbl and Cbl-b both appeared on EGF positive endosomes at the same time (figure 4-6). These data were verified by co-IP, which showed a similar recruitment pattern of c-Cbl and Cbl-b to EGFR over time (figure 4-7). These observations contradict Pennock and Wang (2008), proposing that c-Cbl is recruited earlier than Cbl-b. The weaker signal of c-Cbl compared to Cbl-b on endosomes during live imaging reduced confidence in the analysis and in order to get conclusive results, these experiments need therefore to be repeated. Independent of the tag, however, there appeared to be a weaker signal of c-Cbl than Cbl-b on endosomes after EGF addition (data not shown). IP of GFP-tagged c-Cbl and Cbl-b verified that significantly more EGFR was precipitated with Cbl-b than c-Cbl, indicating that Cbl-b binds a larger proportion of EGFR than c-Cbl.

The observed more efficient interaction between Cbl-b and the EGFR, compared to c-Cbl, has not been demonstrated before. An increased interaction between receptor and Cbl can be due to increased number of Cbl proteins binding to EGFR, which would give the increased signal as observed by live imaging. However, as more Cbl-proteins bind to one EGFR-molecule, the fraction of EGFR precipitated with Cbl would be reduced. Increased interaction of EGFR with Cbl could alternatively be explained by the same amount of Cbl-binding for the two isoforms, but one binding with higher affinity to the EGFR. Precipitation of Cbl might then give an increased fraction of precipitated EGFR, but this would not give any difference in signal intensities for the two isoforms by live imaging. Therefore, these two explanations for increased interaction do not correlate with the findings in this thesis. However, if more EGFR molecules at the PM binds Cbl-b than c-Cbl, meaning not more Cbl molecules per EGFR molecules but a larger portion of EGFR binding Cbl-b than c-Cbl, a larger fraction of EGFR would precipitate with Cbl-b and a stronger signal from Cbl-b would be observed by live imaging. The latter explanation is in accordance with the findings in this thesis. We therefore believe that a larger fraction of EGFR binds Cbl-b than c-Cbl upon EGFR activation. The different efficiencies in recruitment of c-Cbl and Cbl-b to the EGFR might be explained by the ability of Cbl-b to bind ubiquitinated proteins through its UBA

domain (Davies et al., 2004) and thus display higher affinity for the ubiquitinated EGFR. The previous demonstrations from Pennock and Wang (2008) that Cbl-b may have additional binding sites than c-Cbl on the EGFR, might also be a probable explanation for the apparent differences in recruitment of c-Cbl and Cbl-b to EGFR.

Our findings that there was a more efficient interaction between Cbl-b and EGFR compared to c-Cbl and the fact that Cbl has been demonstrated to increase the EGF-induced phosphorylation of the endosomal ubiquitin-sorting protein Hrs (Stern et al., 2007), prompted us to investigate whether transport of the EGF receptor to Hrs positive endosomes could be different in c-Cbl contra Cbl-b overexpressing cells. Phosphorylation of Hrs is important for correct EGFR degradation (Haugen et al., 2013) and alterations in the trafficking pattern might thus affect the rate of EGF receptor downregulation and degradation. As Cbl increases the EGF-induced phosphorylation of Hrs (Stern et al., 2007), a difference in the trafficking of c-Cbl and Cbl-b might influence the phosphorylation of Hrs. The notion that both Cbl and Hrs are associated with the adaptor protein CIN85 (Ronning et al., 2011; Soubeyran et al., 2002), might open the possibility that Cbl somehow regulate phosphorylation of Hrs through CIN85.

We investigated the intracellular trafficking of c-Cbl and Cbl-b to early endosomes, by transiently cotransfecting HeLa and HeLa Ii cells with either EGFP-c-Cbl or EGFP-Cbl-b together with RFP-Hrs, where Hrs was used as a marker for early endosomes (figure 4-8 and 4-9). Quantifications of Hrs-transfected cells (figure 4-9 and 4-11 A and B) showed the same pattern in the colocalization of c-Cbl and Cbl-b with EGF compared to in cells cotransfected with c-Cbl and Cbl-b (figure 4-6). A weaker signal from c-Cbl than Cbl-b was observed in both Hrs-transfected cells upon stimulation with EGF, as observed in cells cotransfected with c-Cbl and Cbl-b. The somewhat different curves of the colocalization of c-Cbl and EGF in Hrs transfected cells compared to cells cotransfected with c-Cbl and Cbl-b, could be explained by the weaker c-Cbl signal in cells cotransfected with c-Cbl and Cbl-b. The colocalization pattern of both c-Cbl and Cbl-b with Hrs positive endosomes appeared to be quite similar (figure 4-9 and 4-11 C and D). Likewise, colocalization of Hrs and EGF started after 4 minutes in cells overexpressing either c-Cbl or Cbl-b (figure 4-9 and 4-11 E and F). Together, these analysis indicated that both c-Cbl and Cbl-b appear to follow the same trafficking pattern regarding recruitment to EGFR and the transport to Hrs positive endosomes.

An interesting note is the analysis of the live imaging at longer time points. Analysis of the experiment with cells cotransfected with DsRed-c-Cbl and EGFP-Cbl-b (supplementary figure 2, movie S1) shows that both c-Cbl and Cbl-b have a peak of colocalization with EGF after 15 minutes, followed by a drop in colocalization when it comes to Cbl-b and EGF. Further, analysis of cells cotransfected with EGFP-c-Cbl and RFP-Hrs (supplementary figure 3, movie S2) demonstrates that colocalization of c-Cbl and EGF had the same peak as colocalization with EGF and Hrs. While there is a decline in c-Cbl colocalizing with EGF and Hrs, there is a prolonged colocalization with EGF and Hrs. This might indicate a transport of EGFR into ILV in MVBs, which is as expected. A similar drop in c-Cbl and EGF colocalization could not be detected in cells cotransfected with c-Cbl and Cbl-b. However, in the movie of the cells co-transfected with c-Cbl and Cbl-b, the c-Cbl signal on endosomes is very weak and considering that these movies are based on one experiment each and with overexpression of different proteins, these experiments must be repeated in order to be able to detect any clear pattern. Nevertheless, the imaging experiments together with the results from the coprecipitations of Cbl and EGFR, contradicts Pennock and Wang (2008), stating that Cbl-b is recruited later than c-Cbl and shows somewhat prolonged association with EGFR after a decline in c-Cbl association.

Taken together, the results in this thesis indicate that Cbl-b is more efficiently recruited to the EGF receptor. However, both c-Cbl and Cbl-b seem to follow the same trafficking pattern both regarding the recruitment to EGFR and the trafficking to early endosomes.

6 Future perspectives

In this study, we have found that Cbl-b is more efficiently recruited to the EGFR than c-Cbl, but this does not appear to affect the intracellular trafficking of the EGFR at early time points. Therefore, further questions remain as to whether there are any differences in the activity of c-Cbl and Cbl-b at later time points. As knockout of one of them does not seem to affect EGFR trafficking (Pennock and Wang, 2008), it can be speculated if the more efficient recruitment of Cbl-b could affect the half-life of signaling proteins rather than affecting EGFR trafficking. The cause for the efficient recruitment of Cbl-b to EGFR needs to be clarified and it would be interesting to investigate its binding sites. A possible approach may be to mutate tyrosines in EGFR upstream of the deletion sites in the paper from Pennock and Wang (2008) and delete the UBA domain in Cbl-b. Lastly, we would like to investigate the late effects of c-Cbl contra Cbl-b overexpression on EGFR, by comparing EGFR degradation efficiency and by measuring growth and duration of signaling.

Unfortunately, we were not able to get long timecourse movies of cells cotransfected with Cbl-b and Hrs as these cells were very sensitive to imaging. In cells cotransfected with c-Cbl and Cbl-b, and c-Cbl and Hrs, the patterns somewhat contradicted each other as c-Cbl seemed to disappear from endosomes after 11 minutes of EGF addition, while in c-Cbl and Cbl-b co-transfected cells c-Cbl still colocalized with EGF after 87 minutes. As the imaging results presented in this thesis are only based on one film in each experiment, more experiments for each condition using only one cell line is needed to make definite conclusions. Also, the cotransfection of Cbl-b and Hrs must be optimalized to get longer movies.

Further, since both c-Cbl and Cbl-b appear to colocalize with Hrs positive endosomes at the same time, it would be of great advantage to be able to optimalize live imaging with Cbl on Ii induced Hrs positive enlarged endosomes to investigate if they might affect the localization of EGF and Cbl on distinct microdomains on the Hrs positive endosomes differently.Cbl has been shown to increase EGFR induced phosphorylation of Hrs and preliminary results showed that both Cbl-proteins induce increased Hrs phosphorylation upon EGFR activation. These experiments need to be optimalized, but it would be very interesting to investigate whether the more efficient Cbl-b recuitment affects Hrs function through phosphorylation, as this modification is important for correct EGFR trafficking.

7 References

Alber, T. 1992. Structure of the leucine zipper. *Curr Opin Genet Dev*. 2:205-210.

Babst, M., D.J. Katzmann, E.J. Estepa-Sabal, T. Meerloo, and S.D. Emr. 2002a. Escrt-III: an endosome-associated heterooligomeric protein complex required for mvb sorting. *Dev Cell*. 3:271-282.

Babst, M., D.J. Katzmann, W.B. Snyder, B. Wendland, and S.D. Emr. 2002b. Endosome-associated complex, ESCRT-II, recruits transport machinery for protein sorting at the multivesicular body. *Dev Cell*. 3:283-289.

Bache, K.G., A. Brech, A. Mehlum, and H. Stenmark. 2003. Hrs regulates multivesicular body formation via ESCRT recruitment to endosomes. *J Cell Biol*. 162:435-442.

Bachmaier, K., C. Krawczyk, I. Kozieradzki, Y.Y. Kong, T. Sasaki, A. Oliveira-dos-Santos, S. Mariathasan, D. Bouchard, A. Wakeham, A. Itie, J. Le, P.S. Ohashi, I. Sarosi, H. Nishina, S. Lipkowitz, and J.M. Penninger. 2000. Negative regulation of lymphocyte activation and autoimmunity by the molecular adaptor Cbl-b. *Nature*. 403:211-216.

Badger-Brown, K.M., L.C. Gillis, M.L. Bailey, J.M. Penninger, and D.L. Barber. 2012. CBL-B is required for leukemogenesis mediated by BCR-ABL through negative regulation of bone marrow homing. *Leukemia*.

Baulida, J., M.H. Kraus, M. Alimandi, P.P. Di Fiore, and G. Carpenter. 1996. All ErbB receptors other than the epidermal growth factor receptor are endocytosis impaired. *J Biol Chem*. 271:5251-5257.

Bazley, L.A., and W.J. Gullick. 2005. The epidermal growth factor receptor family. *Endocr Relat Cancer*. 12 Suppl 1:S17-27.

Blake, T.J., M. Shapiro, H.C. Morse, 3rd, and W.Y. Langdon. 1991. The sequences of the human and mouse c-cbl proto-oncogenes show v-cbl was generated by a large truncation encompassing a proline-rich domain and a leucine zipper-like motif. *Oncogene*. 6:653-657.

Busch, S.J., and P. Sassone-Corsi. 1990. Dimers, leucine zippers and DNA-binding domains. *Trends Genet*. 6:36-40.

Campbell, R.E., O. Tour, A.E. Palmer, P.A. Steinbach, G.S. Baird, D.A. Zacharias, and R.Y. Tsien. 2002. A monomeric red fluorescent protein. *Proc Natl Acad Sci U S A*. 99:7877-7882.

Carpenter, G., and S. Cohen. 1979. Epidermal growth factor. *Annu Rev Biochem*. 48:193-216.

Casaletto, J.B., and A.I. McClatchey. 2012. Spatial regulation of receptor tyrosine kinases in development and cancer. *Nat Rev Cancer*. 12:387-400.

Chiang, Y.J., H.K. Kole, K. Brown, M. Naramura, S. Fukuhara, R.J. Hu, I.K. Jang, J.S. Gutkind, E. Shevach, and H. Gu. 2000. Cbl-b regulates the CD28 dependence of T-cell activation. *Nature*. 403:216-220.

Davies, G.C., S.A. Ettenberg, A.O. Coats, M. Mussante, S. Ravichandran, J. Collins, M.M. Nau, and S. Lipkowitz. 2004. Cbl-b interacts with ubiquitinated proteins; differential functions of the UBA domains of c-Cbl and Cbl-b. *Oncogene*. 23:7104-7115.

Doherty, G.J., and H.T. McMahon. 2009. Mechanisms of endocytosis. *Annu Rev Biochem*. 78:857-902.

El Chami, N., F. Ikhlef, K. Kaszas, S. Yakoub, E. Tabone, B. Siddeek, S. Cunha, C. Beaudoin, L. Morel, M. Benahmed, and D.C. Regnier. 2005. Androgen-dependent apoptosis in male germ cells is regulated through the proto-oncoprotein Cbl. *J Cell Biol*. 171:651-661.

Endres, N.F., K. Engel, R. Das, E. Kovacs, and J. Kuriyan. 2011. Regulation of the catalytic activity of the EGF receptor. *Curr Opin Struct Biol*. 21:777-784.

Ettenberg, S.A., A. Magnifico, M. Cuello, M.M. Nau, Y.R. Rubinstein, Y. Yarden, A.M. Weissman, and S. Lipkowitz. 2001. Cbl-b-dependent coordinated degradation of the epidermal growth factor receptor signaling complex. *J Biol Chem*. 276:27677-27684.

Ettenberg, S.A., Y.R. Rubinstein, P. Banerjee, M.M. Nau, M.M. Keane, and S. Lipkowitz. 1999. cbl-b inhibits EGF-receptor-induced apoptosis by enhancing ubiquitination and degradation of activated receptors. *Mol Cell Biol Res Commun*. 2:111-118.

Freemont, P.S., I.M. Hanson, and J. Trowsdale. 1991. A novel cysteine-rich sequence motif. *Cell*. 64:483-484.

Futter, C.E., A. Pearse, L.J. Hewlett, and C.R. Hopkins. 1996. Multivesicular endosomes containing internalized EGF-EGF receptor complexes mature and then fuse directly with lysosomes. *J Cell Biol*. 132:1011-1023.

Goh, L.K., F. Huang, W. Kim, S. Gygi, and A. Sorkin. 2010. Multiple mechanisms collectively regulate clathrin-mediated endocytosis of the epidermal growth factor receptor. *J Cell Biol*. 189:871-883.

Goldknopf, I.L., M.F. French, R. Musso, and H. Busch. 1977. Presence of protein A24 in rat liver nucleosomes. *Proc Natl Acad Sci U S A*. 74:5492-5495.

Gorgoulis, V., D. Aninos, P. Mikou, P. Kanavaros, A. Karameris, J. Joardanoglou, A. Rasidakis, M. Veslemes, B. Ozanne, and D.A. Spandidos. 1992. Expression of EGF, TGF-alpha and EGFR in squamous cell lung carcinomas. *Anticancer Res*. 12:1183-1187.

Griffiths, E.K., O. Sanchez, P. Mill, C. Krawczyk, C.V. Hojilla, E. Rubin, M.M. Nau, R. Khokha, S. Lipkowitz, C.C. Hui, and J.M. Penninger. 2003. Cbl-3-deficient mice exhibit normal epithelial development. *Mol Cell Biol*. 23:7708-7718.

Grovdal, L.M., E. Stang, A. Sorkin, and I.H. Madshus. 2004. Direct interaction of Cbl with pTyr 1045 of the EGF receptor (EGFR) is required to sort the EGFR to lysosomes for degradation. *Exp Cell Res*. 300:388-395.

Haglund, K., and I. Dikic. 2012. The role of ubiquitylation in receptor endocytosis and endosomal sorting. *J Cell Sci*. 125:265-275.

Haglund, K., S. Sigismund, S. Polo, I. Szymkiewicz, P.P. Di Fiore, and I. Dikic. 2003. Multiple monoubiquitination of RTKs is sufficient for their endocytosis and degradation. *Nat Cell Biol*. 5:461-466.

Haugen, L.H., F.M. Skjeldal, T. Bergeland, and O. Bakke. 2013. Receptor tyrosine kinases control their own degradation by regulating the phosphorylation and endosomal binding kinetics of Eps15 and Hrs. *Nat Cell Biol*.

Hershko, A., A. Ciechanover, H. Heller, A.L. Haas, and I.A. Rose. 1980. Proposed role of ATP in protein breakdown: conjugation of protein with multiple chains of the polypeptide of ATP-dependent proteolysis. *Proc Natl Acad Sci U S A*. 77:1783-1786.

Hershko, A., H. Heller, S. Elias, and A. Ciechanover. 1983. Components of ubiquitin-protein ligase system. Resolution, affinity purification, and role in protein breakdown. *J Biol Chem*. 258:8206-8214.

Huang, C. 2010. Roles of E3 ubiquitin ligases in cell adhesion and migration. *Cell Adh Migr*. 4:10-18.

Huang, F., D. Kirkpatrick, X. Jiang, S. Gygi, and A. Sorkin. 2006. Differential regulation of EGF receptor internalization and degradation by multiubiquitination within the kinase domain. *Mol Cell*. 21:737-748.

Huang, F., and A. Sorkin. 2005. Growth factor receptor binding protein 2-mediated recruitment of the RING domain of Cbl to the epidermal growth factor receptor is essential and sufficient to support receptor endocytosis. *Mol Biol Cell*. 16:1268-1281.

Huibregtse, J.M., M. Scheffner, S. Beaudenon, and P.M. Howley. 1995. A family of proteins structurally and functionally related to the E6-AP ubiquitin-protein ligase. *Proc Natl Acad Sci U S A*. 92:2563-2567.

Husnjak, K., and I. Dikic. 2012. Ubiquitin-binding proteins: decoders of ubiquitin-mediated cellular functions. *Annu Rev Biochem*. 81:291-322.

Hynes, N.E., and G. MacDonald. 2009. ErbB receptors and signaling pathways in cancer. *Curr Opin Cell Biol*. 21:177-184.

Irish, J.C., and A. Bernstein. 1993. Oncogenes in head and neck cancer. *Laryngoscope*. 103:42-52.

Jeon, M.S., A. Atfield, K. Venuprasad, C. Krawczyk, R. Sarao, C. Elly, C. Yang, S. Arya, K. Bachmaier, L. Su, D. Bouchard, R. Jones, M. Gronski, P. Ohashi, T. Wada, D. Bloom, C.G. Fathman, Y.C. Liu, and J.M. Penninger. 2004. Essential role of the E3 ubiquitin ligase Cbl-b in T cell anergy induction. *Immunity*. 21:167-177.

Joazeiro, C.A., S.S. Wing, H. Huang, J.D. Leverson, T. Hunter, and Y.C. Liu. 1999. The tyrosine kinase negative regulator c-Cbl as a RING-type, E2-dependent ubiquitin-protein ligase. *Science*. 286:309-312.

Kassenbrock, C.K., and S.M. Anderson. 2004. Regulation of ubiquitin protein ligase activity in c-Cbl by phosphorylation-induced conformational change and constitutive activation by tyrosine to glutamate point mutations. *J Biol Chem*. 279:28017-28027.

Katzmann, D.J., M. Babst, and S.D. Emr. 2001. Ubiquitin-dependent sorting into the multivesicular body pathway requires the function of a conserved endosomal protein sorting complex, ESCRT-I. *Cell*. 106:145-155.

Keane, M.M., S.A. Ettenberg, M.M. Nau, P. Banerjee, M. Cuello, J. Penninger, and S. Lipkowitz. 1999. cbl-3: a new mammalian cbl family protein. *Oncogene*. 18:3365-3375.

Keane, M.M., O.M. Rivero-Lezcano, J.A. Mitchell, K.C. Robbins, and S. Lipkowitz. 1995. Cloning and characterization of cbl-b: a SH3 binding protein with homology to the c-cbl proto-oncogene. *Oncogene*. 10:2367-2377.

Kim, J.H., K. Kushiro, N.A. Graham, and A.R. Asthagiri. 2009. Tunable interplay between epidermal growth factor and cell-cell contact governs the spatial dynamics of epithelial growth. *Proc Natl Acad Sci U S A*. 106:11149-11153.

Komander, D., M.J. Clague, and S. Urbe. 2009. Breaking the chains: structure and function of the deubiquitinases. *Nat Rev Mol Cell Biol*. 10:550-563.

Kowanetz, K., I. Szymkiewicz, K. Haglund, M. Kowanetz, K. Husnjak, J.D. Taylor, P. Soubeyran, U. Engstrom, J.E. Ladbury, and I. Dikic. 2003. Identification of a novel proline-arginine motif involved in CIN85-dependent clustering of Cbl and down-regulation of epidermal growth factor receptors. *J Biol Chem*. 278:39735-39746.

Krasinskas, A.M. 2011. EGFR Signaling in Colorectal Carcinoma. *Patholog Res Int*. 2011:932932.

Lai, W.H., P.H. Cameron, J.J. Doherty, 2nd, B.I. Posner, and J.J. Bergeron. 1989. Ligand-mediated autophosphorylation activity of the epidermal growth factor receptor during internalization. *J Cell Biol*. 109:2751-2760.

Langdon, W.Y., J.W. Hartley, S.P. Klinken, S.K. Ruscetti, and H.C. Morse, 3rd. 1989a. v-cbl, an oncogene from a dual-recombinant murine retrovirus that induces early B-lineage lymphomas. *Proc Natl Acad Sci U S A*. 86:1168-1172.

Langdon, W.Y., C.D. Hyland, R.J. Grumont, and H.C. Morse, 3rd. 1989b. The c-cbl proto-oncogene is preferentially expressed in thymus and testis tissue and encodes a nuclear protein. *J Virol*. 63:5420-5424.

Lemmon, M.A., and J. Schlessinger. 2010. Cell signaling by receptor tyrosine kinases. *Cell*. 141:1117-1134.

Levkowitz, G., H. Waterman, S.A. Ettenberg, M. Katz, A.Y. Tsygankov, I. Alroy, S. Lavi, K. Iwai, Y. Reiss, A. Ciechanover, S. Lipkowitz, and Y. Yarden. 1999. Ubiquitin ligase activity and tyrosine phosphorylation underlie suppression of growth factor signaling by c-Cbl/Sli-1. *Mol Cell*. 4:1029-1040.

McMahon, H.T., and E. Boucrot. 2011. Molecular mechanism and physiological functions of clathrin-mediated endocytosis. *Nat Rev Mol Cell Biol*. 12:517-533.

Meisner, H., and M.P. Czech. 1995. Coupling of the proto-oncogene product c-Cbl to the epidermal growth factor receptor. *J Biol Chem*. 270:25332-25335.

Meng, W., S. Sawasdikosol, S.J. Burakoff, and M.J. Eck. 1999. Structure of the amino-terminal domain of Cbl complexed to its binding site on ZAP-70 kinase. *Nature*. 398:84-90.

Miettinen, P.J., J.E. Berger, J. Meneses, Y. Phung, R.A. Pedersen, Z. Werb, and R. Derynck. 1995. Epithelial immaturity and multiorgan failure in mice lacking epidermal growth factor receptor. *Nature*. 376:337-341.

Mohapatra, B., G. Ahmad, S. Nadeau, N. Zutshi, W. An, S. Scheffe, L. Dong, D. Feng, B. Goetz, P. Arya, T.A. Bailey, N. Palermo, G.E. Borgstahl, A. Natarajan, S.M. Raja, M. Naramura, V. Band, and H. Band. 2013. Protein tyrosine kinase regulation by ubiquitination: critical roles of Cbl-family ubiquitin ligases. *Biochim Biophys Acta*. 1833:122-139.

Mosesson, Y., K. Shtiegman, M. Katz, Y. Zwang, G. Vereb, J. Szollosi, and Y. Yarden. 2003. Endocytosis of receptor tyrosine kinases is driven by monoubiquitylation, not polyubiquitylation. *J Biol Chem*. 278:21323-21326.

Murphy, M.A., R.G. Schnall, D.J. Venter, L. Barnett, I. Bertoncello, C.B. Thien, W.Y. Langdon, and D.D. Bowtell. 1998. Tissue hyperplasia and enhanced T-cell signalling via ZAP-70 in c-Cbl-deficient mice. *Mol Cell Biol*. 18:4872-4882.

Naramura, M., I.K. Jang, H. Kole, F. Huang, D. Haines, and H. Gu. 2002. c-Cbl and Cbl-b regulate T cell responsiveness by promoting ligand-induced TCR down-modulation. *Nat Immunol*. 3:1192-1199.

Naramura, M., H.K. Kole, R.J. Hu, and H. Gu. 1998. Altered thymic positive selection and intracellular signals in Cbl-deficient mice. *Proc Natl Acad Sci U S A*. 95:15547-15552.

Naramura, M., N. Nandwani, H. Gu, V. Band, and H. Band. 2010. Rapidly fatal myeloproliferative disorders in mice with deletion of Casitas B-cell lymphoma (Cbl) and Cbl-b in hematopoietic stem cells. *Proc Natl Acad Sci U S A*. 107:16274-16279.

Olayioye, M.A., D. Graus-Porta, R.R. Beerli, J. Rohrer, B. Gay, and N.E. Hynes. 1998. ErbB-1 and ErbB-2 acquire distinct signaling properties dependent upon their dimerization partner. *Mol Cell Biol*. 18:5042-5051.

Pennock, S., and Z. Wang. 2008. A tale of two Cbls: interplay of c-Cbl and Cbl-b in epidermal growth factor receptor downregulation. *Mol Cell Biol*. 28:3020-3037.
Progida, C., M.S. Nielsen, G. Koster, C. Bucci, and O. Bakke. 2012. Dynamics of Rab7b-dependent transport of sorting receptors. *Traffic*. 13:1273-1285.
Raiborg, C., K.G. Bache, D.J. Gillooly, I.H. Madshus, E. Stang, and H. Stenmark. 2002. Hrs sorts ubiquitinated proteins into clathrin-coated microdomains of early endosomes. *Nat Cell Biol*. 4:394-398.
Raiborg, C., and H. Stenmark. 2009. The ESCRT machinery in endosomal sorting of ubiquitylated membrane proteins. *Nature*. 458:445-452.
Rathinam, C., C.B. Thien, R.A. Flavell, and W.Y. Langdon. 2010. Myeloid leukemia development in c-Cbl RING finger mutant mice is dependent on FLT3 signaling. *Cancer Cell*. 18:341-352.
Rathinam, C., C.B. Thien, W.Y. Langdon, H. Gu, and R.A. Flavell. 2008. The E3 ubiquitin ligase c-Cbl restricts development and functions of hematopoietic stem cells. *Genes Dev*. 22:992-997.
Roepstorff, K., M.V. Grandal, L. Henriksen, S.L. Knudsen, M. Lerdrup, L. Grovdal, B.M. Willumsen, and B. van Deurs. 2009. Differential effects of EGFR ligands on endocytic sorting of the receptor. *Traffic*. 10:1115-1127.
Ronning, S.B., N.M. Pedersen, I.H. Madshus, and E. Stang. 2011. CIN85 regulates ubiquitination and degradative endosomal sorting of the EGF receptor. *Exp Cell Res*. 317:1804-1816.
Ryan, P.E., G.C. Davies, M.M. Nau, and S. Lipkowitz. 2006. Regulating the regulator: negative regulation of Cbl ubiquitin ligases. *Trends Biochem Sci*. 31:79-88.
Schlessinger, J., A.B. Schreiber, A. Levi, I. Lax, T. Libermann, and Y. Yarden. 1983. Regulation of cell proliferation by epidermal growth factor. *CRC Crit Rev Biochem*. 14:93-111.
Scita, G., and P.P. Di Fiore. 2010. The endocytic matrix. *Nature*. 463:464-473.
Shaner, N.C., P.A. Steinbach, and R.Y. Tsien. 2005. A guide to choosing fluorescent proteins. *Nat Methods*. 2:905-909.
Shao, Y., C. Yang, C. Elly, and Y.C. Liu. 2004. Differential regulation of the B cell receptor-mediated signaling by the E3 ubiquitin ligase Cbl. *J Biol Chem*. 279:43646-43653.
Sibilia, M., and E.F. Wagner. 1995. Strain-dependent epithelial defects in mice lacking the EGF receptor. *Science*. 269:234-238.
Sigismund, S., S. Confalonieri, A. Ciliberto, S. Polo, G. Scita, and P.P. Di Fiore. 2012. Endocytosis and signaling: cell logistics shape the eukaryotic cell plan. *Physiol Rev*. 92:273-366.
Sigismund, S., T. Woelk, C. Puri, E. Maspero, C. Tacchetti, P. Transidico, P.P. Di Fiore, and S. Polo. 2005. Clathrin-independent endocytosis of ubiquitinated cargos. *Proc Natl Acad Sci U S A*. 102:2760-2765.
Sorkin, A., and G. Carpenter. 1991. Dimerization of internalized epidermal growth factor receptors. *J Biol Chem*. 266:23453-23460.
Sorkin, A., and M. von Zastrow. 2009. Endocytosis and signalling: intertwining molecular networks. *Nat Rev Mol Cell Biol*. 10:609-622.
Soubeyran, P., K. Kowanetz, I. Szymkiewicz, W.Y. Langdon, and I. Dikic. 2002. Cbl-CIN85-endophilin complex mediates ligand-induced downregulation of EGF receptors. *Nature*. 416:183-187.
Stern, K.A., G.D. Visser Smit, T.L. Place, S. Winistorfer, R.C. Piper, and N.L. Lill. 2007. Epidermal growth factor receptor fate is controlled by Hrs tyrosine phosphorylation sites that regulate Hrs degradation. *Mol Cell Biol*. 27:888-898.

Szymkiewicz, I., K. Kowanetz, P. Soubeyran, A. Dinarina, S. Lipkowitz, and I. Dikic. 2002. CIN85 participates in Cbl-b-mediated down-regulation of receptor tyrosine kinases. *J Biol Chem*. 277:39666-39672.

Thien, C.B., and W.Y. Langdon. 2005. c-Cbl and Cbl-b ubiquitin ligases: substrate diversity and the negative regulation of signalling responses. *Biochem J*. 391:153-166.

Threadgill, D.W., A.A. Dlugosz, L.A. Hansen, T. Tennenbaum, U. Lichti, D. Yee, C. LaMantia, T. Mourton, K. Herrup, R.C. Harris, and et al. 1995. Targeted disruption of mouse EGF receptor: effect of genetic background on mutant phenotype. *Science*. 269:230-234.

Vermeer, P.D., L.A. Einwalter, T.O. Moninger, T. Rokhlina, J.A. Kern, J. Zabner, and M.J. Welsh. 2003. Segregation of receptor and ligand regulates activation of epithelial growth factor receptor. *Nature*. 422:322-326.

Waterman, H., M. Katz, C. Rubin, K. Shtiegman, S. Lavi, A. Elson, T. Jovin, and Y. Yarden. 2002. A mutant EGF-receptor defective in ubiquitylation and endocytosis unveils a role for Grb2 in negative signaling. *EMBO J*. 21:303-313.

Wieduwilt, M.J., and M.M. Moasser. 2008. The epidermal growth factor receptor family: biology driving targeted therapeutics. *Cell Mol Life Sci*. 65:1566-1584.

Woelk, T., S. Sigismund, L. Penengo, and S. Polo. 2007. The ubiquitination code: a signalling problem. *Cell Div*. 2:11.

Wong, A.J., J.M. Ruppert, S.H. Bigner, C.H. Grzeschik, P.A. Humphrey, D.S. Bigner, and B. Vogelstein. 1992. Structural alterations of the epidermal growth factor receptor gene in human gliomas. *Proc Natl Acad Sci U S A*. 89:2965-2969.

Wright, M.H., I. Berlin, and P.D. Nash. 2011. Regulation of endocytic sorting by ESCRT-DUB-mediated deubiquitination. *Cell Biochem Biophys*. 60:39-46.

Xie, Y., and A. Varshavsky. 1999. The E2-E3 interaction in the N-end rule pathway: the RING-H2 finger of E3 is required for the synthesis of multiubiquitin chain. *EMBO J*. 18:6832-6844.

Yano, S., K. Kondo, M. Yamaguchi, G. Richmond, M. Hutchison, A. Wakeling, S. Averbuch, and P. Wadsworth. 2003. Distribution and function of EGFR in human tissue and the effect of EGFR tyrosine kinase inhibition. *Anticancer Res*. 23:3639-3650.

Yarden, Y., and J. Schlessinger. 1987a. Epidermal growth factor induces rapid, reversible aggregation of the purified epidermal growth factor receptor. *Biochemistry*. 26:1443-1451.

Yarden, Y., and J. Schlessinger. 1987b. Self-phosphorylation of epidermal growth factor receptor: evidence for a model of intermolecular allosteric activation. *Biochemistry*. 26:1434-1442.

Yoon, C.H., J. Lee, G.D. Jongeward, and P.W. Sternberg. 1995. Similarity of sli-1, a regulator of vulval development in C. elegans, to the mammalian proto-oncogene c-cbl. *Science*. 269:1102-1105.

Zhang, J., Y.J. Chiang, R.J. Hodes, and R.P. Siraganian. 2004. Inactivation of c-Cbl or Cbl-b differentially affects signaling from the high affinity IgE receptor. *J Immunol*. 173:1811-1818.

Supplementary

Figure S1

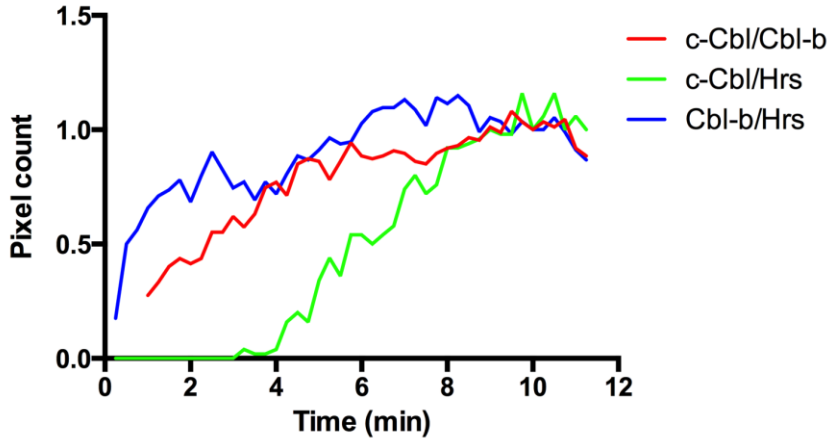

Figure S1. Count of pixels representing Alexa 647-EGF positive structures.
Pixel count of Alexa 647-EGF structures in cells cotransfected with DsRed-c-Cbl and EGFP-Cbl-b (movie S1) **(Red),** EGFP-c-Cbl and RFP-Hrs (movie S2) **(Green)**, and EGFP-Cbl-b and RFP-Hrs (movie S3) **(Blue).** All images were analyzed in ImageJ.

Figure S2

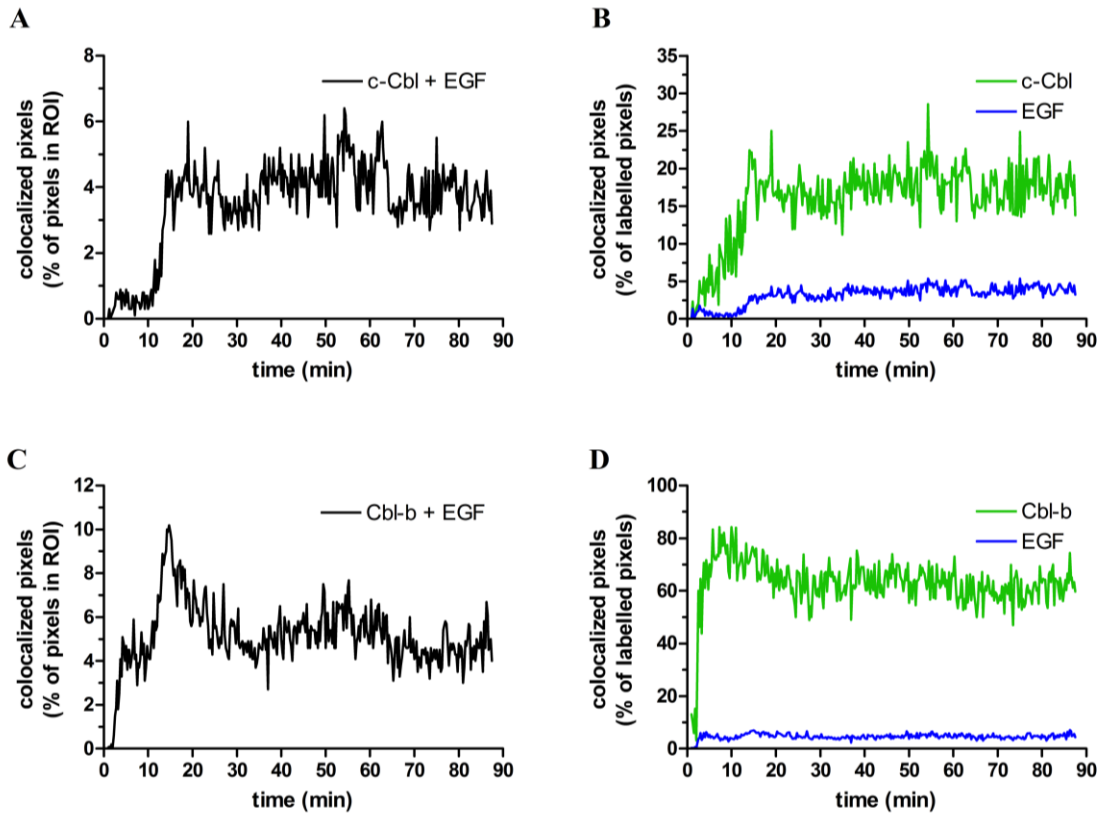

Figure S2. Quantification of colocalization of c-Cbl and EGF, and Cbl-b and EGF at longer time points. Quantification of live imaging in figure 4-5 (movie S1), analyzed in ImageJ.

A and **C**: Percentage of colocalized pixels measured as number of pixels showing colocalization of c-Cbl and EGF (**A)** or Cbl-b and EGF (**C)** out of total number of pixels in ROI. **B** and **D**: Percentage colocalization meaured as fraction of colocalized pixels relative to the total number of c-Cbl or EGF (**B)** pixels or number of Cbl-b or EGF (**D)** pixels in the ROI. The analysis was based on one experiment.

Figure S3

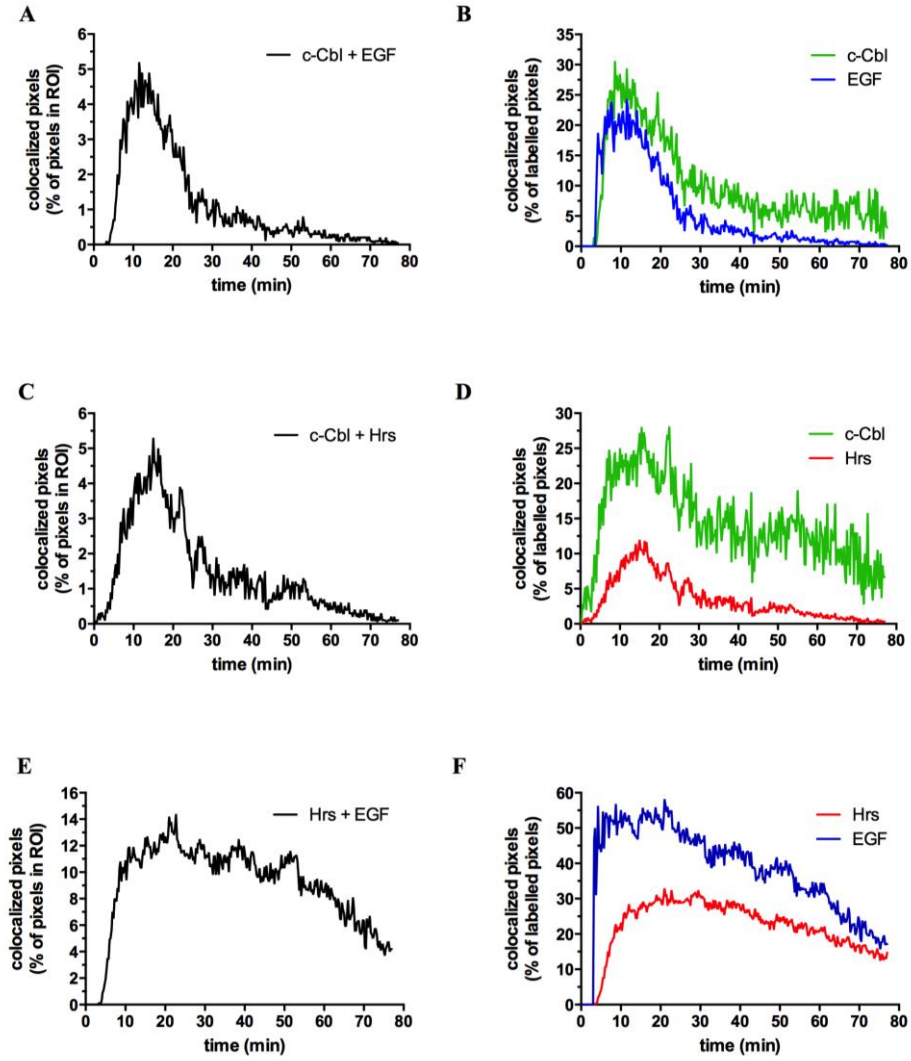

Figure S3. Quantification of colocalization of c-Cbl and EGF, c-Cbl and Hrs and Hrs and EGF at longer time points.

Quantification of live imaging in figure 4-8 (movie S2), analyzed in ImageJ.

A: Percentage colocalization of c-Cbl and EGF in ROI. **B:** Percentage colocalization relative to the amount of c-Cbl or EGF in the ROI. **C:** Percentage colocalization of c-Cbl and Hrs in ROI. **D:** Percentage colocalization relative to the amount of c-Cbl or Hrs in the ROI. **E:** Percentage colocalization of Hrs and EGF ROI. **F:** Percentage colocalization relative to the amount of Hrs or EGF in the ROI.

.

Table S1: Antibodies

Antibody	Class	Epitope	Purchased from	Concentration for WB	Concentration for IP	Primary (P)/ Secondary (S)
Anti c-Cbl	Rabbit IgG	c-Cbl (human)	Santa Cruz, CA, USA	1:500		P
Anti Cbl-b	Rabbit IgG	Cbl-b (human)	Santa Cruz, CA, USA	1:200		P
Anti Hrs	Rabbit IgG	Hrs (mouse)	Harald Stenmark*	1:1000		P
Anti EGFR	Sheep IgG	EGFR (human)	Fitzgerald, MA, USA	1:10000		P
M-B741	Mouse IgG	Ii C-terminus (all isoforms) (human)	Santa Cruz, CA, USA	1:5000		P
Anti tubulin	Mouse ascites	N-terminus of α-tubulin (various species)	Zymed Laboratories, CA, USA	1:5000		P
Anti GFP	Rabbit		Abcam, Cambridge, UK	1:1000	1µg	P
Sheep anti-mouse IgG HRP-linked	Sheep IgG		GE Healthcare, Buckinghamshire, UK	1:10000		S
Donkey anti-rabbit IgG HRP-linked	Donkey IgG		GE Healthcare, Buckinghamshire, UK	1:10000		S
Rabbit Anti-sheep	Rabbit IgG		Southern Biotech, AL, USA	1:8000		S

** Harald Stenmark, Centre for Cancer Biomedicine, Norwegian Radium Hospital, University of Oslo, Oslo, Norway.*

Table S2: Lysis buffers

Lysis buffer for Western Blot

Ingredients	Concentration
Tris-HCl (pH 6.8)	50 mM
EDTA (pH 8)	5 mM
NaF	30 mM
Sodium pyrophosphate	50 mM
dH_2O	Adjustment to desired volume
0,5 % Nonidet P-40 and 1:100 protease inhibitor (Roche, Basel Switzerland) was added before use	

Lysis buffer for immunoprecipitation

Ingredients	Concentration
Sodium phosphate-buffer (pH 7,2)	0.01 mM
EDTA (pH 8)	10 mM
NaF	30 mM
NaCl	0.15 mM
dH_2O	Adjustment to desired volume
0,5 % Nonidet P-40, 1:100 protease inhibitor (Roche), 1:100 phosphatase inhibitor cocktail (Sigma-Aldrich) and 100 mM n-ethylmaleimide was added before use	

Table S3: Hepes Running buffer (1x)

Ingredients	Concentration
Tris	10 mM
Hepes	35 mM
SDS	3 mM

dH_2O	Adjustment to desired volume

Table S4: Transfer buffer (1x)

Ingredients	Concentration
Glycine	380 mM
Tris	50 mM
Methanol (Sigma-Aldrich)	10 %
dH_2O	Adjustment to desired volume

Table S5: TBS (1x) (pH 7.6)

Ingredients	Concentration
Tris	20 mM
NaCl	0,0137 mM
dH_2O	Adjustment to desired volume

Table S6: Gel loading buffer (6 x) for Western blot

Ingredients	Concentration
Glycerol	30 %
Bromophenol blue	0,3 %
β-mercaptoethanol	24 %
SDS	12 %
dH_2O	Adjustment to desired volume

Table S7: Gel loading buffer (2 x) for immunoprecipitation

Ingredients	Concentration
Glycerol	10 %
Bromophenol blue	0,01 %
β-mercaptoethanol	8 %
SDS	4 %
EDTA (pH 8)	10 mM
Na pyrophosphate	60 mM
NaF	100 mM
Tris-HCl (pH 6,8)	125 mM
dH_2O	Adjustment to desired volume

Supplementary movies

Movie S1: Trafficking of c-Cbl and Cbl-b

HeLa cells were transiently cotransfected with DsRed-c-Cbl and EGFP-Cbl-b and stimulated with 100 ng/ml Alexa 647-tagged EGF under live imaging at 37 °C using Spinning Disc confocal microscopy. **Note**: The movie has a longer time scale than the movie with HeLa Ii cells cotransfected with EGFP-Cbl-b and RFP-Hrs.
Scale bar = 10 μm

Movie S2: Trafficking of c-Cbl and Hrs

HeLa cells were transiently cotransfected with EGFP-c-Cbl and RFP-Hrs at 37 °C over night and stimulated with 100 ng/ml Alexa 647-tagged EGF under live imaging using Spinning Disc confocal microscopy.
Note: The movie has a longer time scale than the movie with HeLa Ii cells cotransfected with EGFP-Cbl-b and RFP-Hrs.
Scale bar = 10 μm

Movie S3: Trafficking of Cbl-b and Hrs

HeLa Ii cells were transiently cotransfected with EGFP-Cbl-b and RFP-Hrs at 37 °C over night and stimulated with 100 ng/ml Alexa 647-tagged EGF under live imaging using Spinning Disc confocal microscopy.
Scale bar = 10 μm

Appendix

Previous master project

Initially, the master project was to study the role of Hrs and Eps15 in intracellular trafficking of the FcεRI, the high affinity receptor for IgE. The study was thought to investigate if Hrs and Eps15 had similar functions in the intracellular trafficking of FcεRI as for the EGF receptor (Haugen et al., 2013). Mast cells (RBL-2H3) were used to study the degranulation response resulting from stimulation of FcεRI with IgE cross bound with allergen. Both degranulation assays, immunoprecipitations, Flow cytometry, live imaging and imaging of fixed cells were applied. Unfortunately, the cells were not responding properly giving contradicting results and there were difficulties finding appropriate antibodies against the subunits of FcεRI in the biochemical experiments. The project was ended september last year after a year with attempts to get trustworthy results.